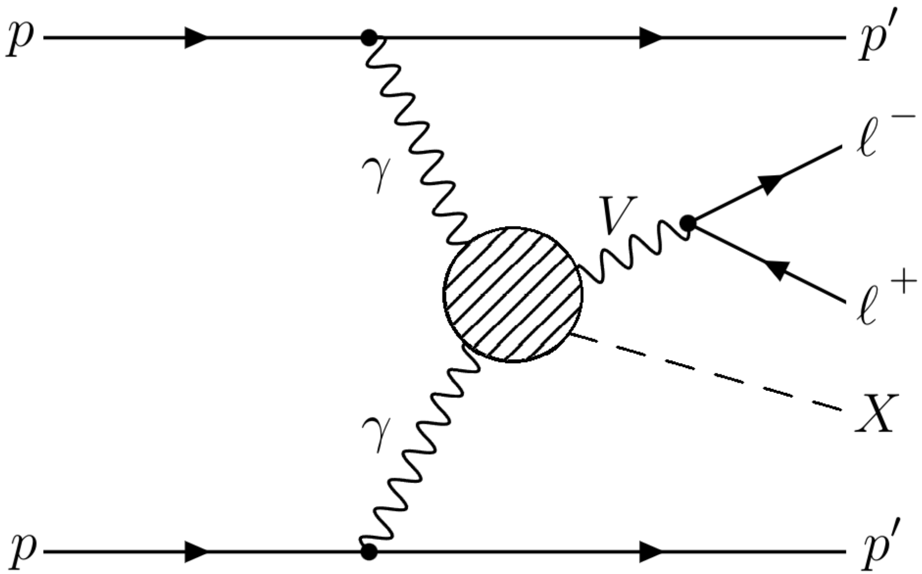

Search for missing mass in proton-tagged dilepton events with the ATLAS detector and the AFP spectrometer

Josh Lomas

University of Birmingham

22/07/2026

Introduction

The **Standard Model** is our best current understanding of the fundamental structure of the Universe

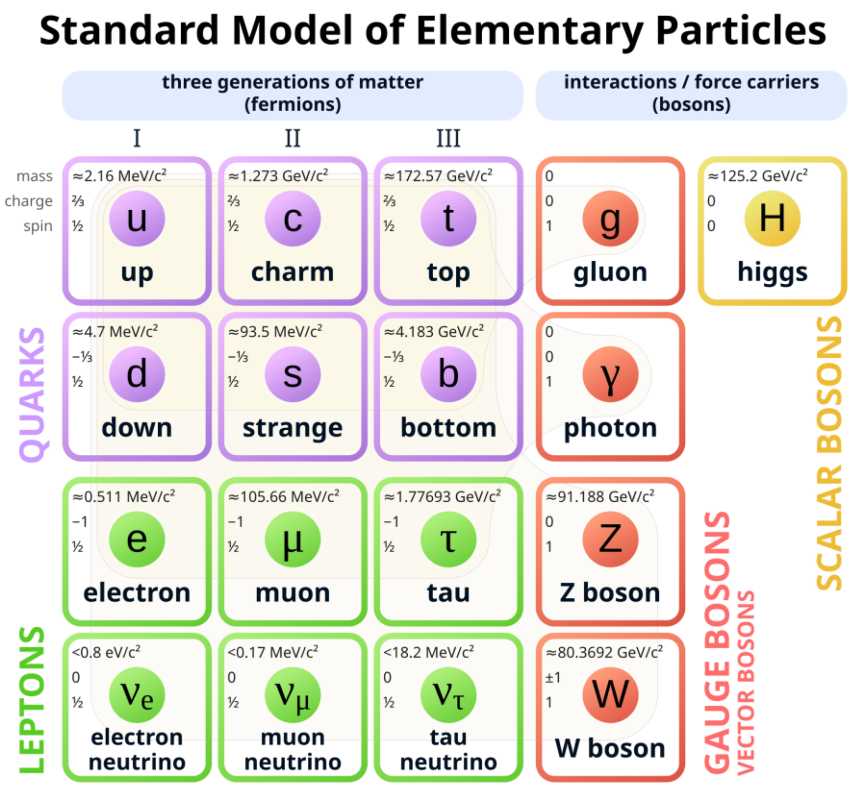

- ✓ Includes all particles so far discovered
- ✓ Incorporates three of the four fundamental forces
- ✓ Explains the mass of particles
- ✓ Agrees with the majority of experimental measurements

However, it falls short in several places, e.g.

- ✗ Why is there more matter than anti-matter?
- ✗ What is dark matter/energy?
- ✗ How does gravity fit in?
- ✗ Do neutrinos have mass?

We need to explore new phase spaces to search for **Beyond the Standard Model** physics

Large Hadron Collider (LHC)

The **largest particle accelerator** ever built

- 26.7 km circumference
- 100 m below the surface of the Swiss-French border at CERN
- **Colliding protons together** at centre-of-mass energies up to $\sqrt{s}$ = 13.6 TeV
- At full capacity, each beam comprises 2,556 bunches of protons, each containing around 10^{11} protons and undergoing **collisions every 25 ns**
- When proton bunches cross over, **multiple proton-proton interactions** occur simultaneously (~40 on average in 2017)
  - ➢ Typically, at most only 1 “event of interest” per bunch crossing
  - ➢ Additional interactions referred to as “**pile-up**”

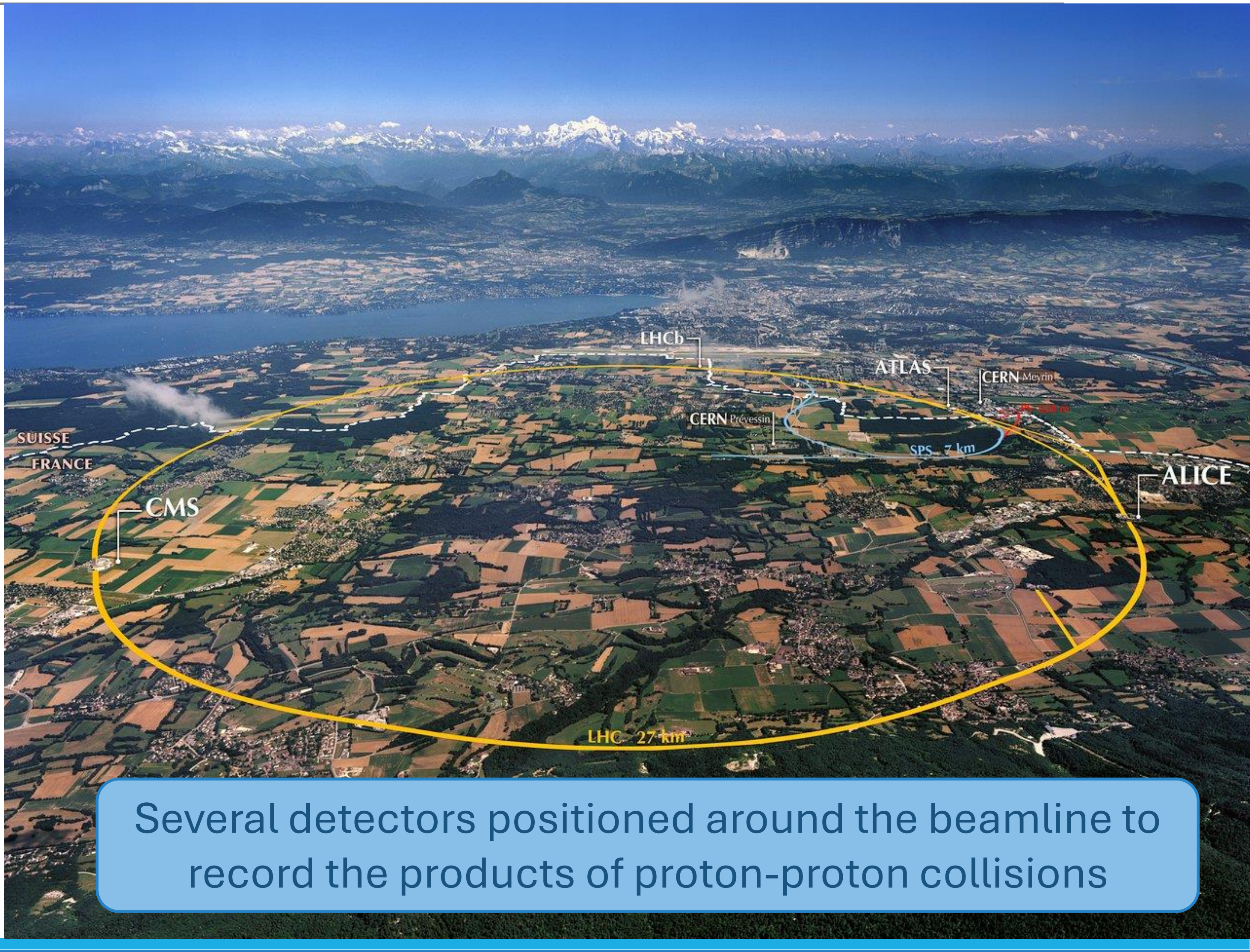

Several detectors positioned around the beamline to record the products of proton-proton collisions

The ATLAS Detector

A Toroidal **L**HC **A**pparatu**S** (**ATLAS**) is one of two large **general-purpose particle detectors** at the LHC

- **Cylindrical design** to cover almost the **entire solid angle** around the interaction point
- Made up of a series of **concentric layers**, each detecting a different component of the interaction products:
  - **Inner Detector** (Pixel, SCT, TRT): measures the trajectories and momenta of charged particles
  - **Calorimeters** (ECal and HCal): measures the energy of EM and hadronic particles, respectively
  - **Muon Spectrometer**: measures the momenta of muons
  - **Solenoid and toroid magnets** to curve charged particle trajectories

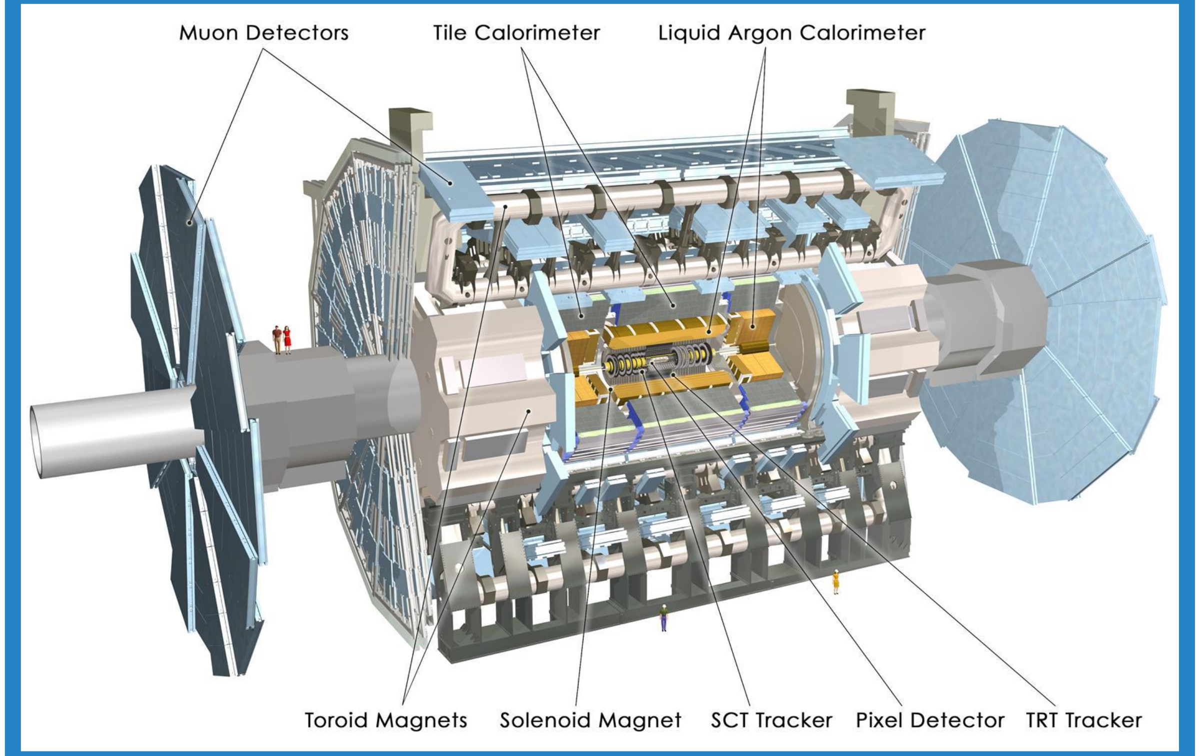

Photon-Photon Collisions

One largely unexplored area of particle physics is **photon-photon collisions**

- At ultra-relativistic speeds (e.g. at the LHC) the EM field around protons is compressed to resemble a flux of photons

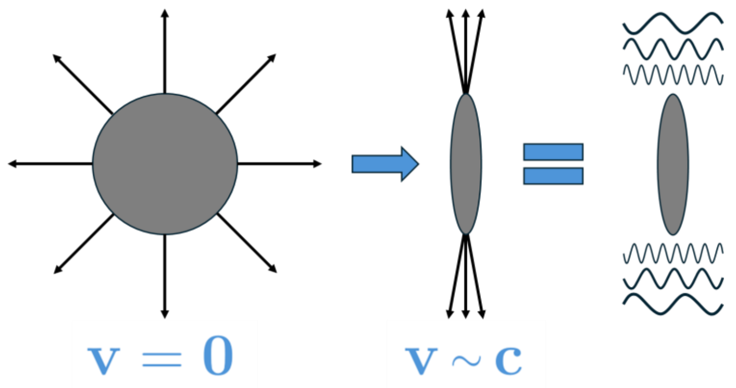

- When protons narrowly miss each other at the ATLAS IP, these photons can interact to yield **central production** of particles
  - Proton quantum numbers are unchanged
  - For low-Q^2 interactions they can **remain intact**
  - Continue down the beam at a scattered angle due to energy loss

Intact and Dissociated Final State Protons

- If both protons remain intact (elastic interaction), central signature is **exclusive**
  - Contains only centrally produced particles (η~0) and outgoing protons (high-η)
  - Leaves **rapidity gap** in low to mid-rapidity region
  - Energy in central production **exactly equal** to energy lost by protons

> If BSM particles are centrally produced and not detected by ATLAS, their mass will be "**missing**" from the central energy predicted by the proton energy loss

- Outgoing protons can become excited and break apart into hadronic showers
  - No longer simple to constrain the energy of the central system

Exclusive process

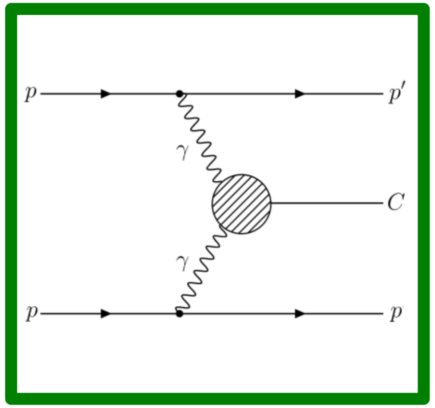

Elastic-elastic (EE)

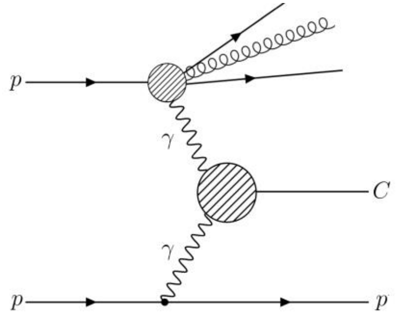

Single dissociative (SD)

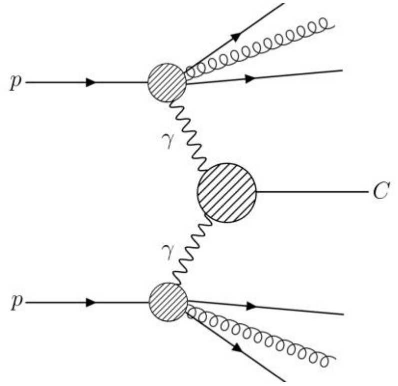

Double dissociative (DD)

Soft-Survival

- Protons can undergo **further interactions** following elastic photon exchange
  - Produces additional particles at low to mid-rapidity "killing" the rapidity gap
  - Probability that this does not happen is parametrised by the **soft-survival probability** $S \leq 1$

- Dependent on momentum transfer Q^2 and properties of central system e.g. dilepton mass for photon-induced dilepton production:

2007.12704

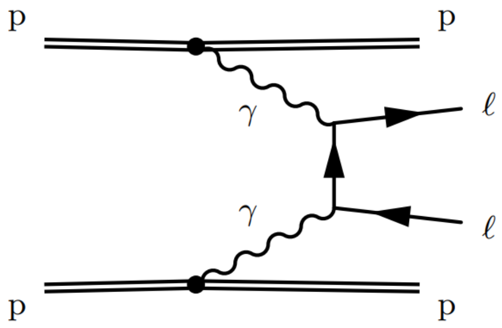

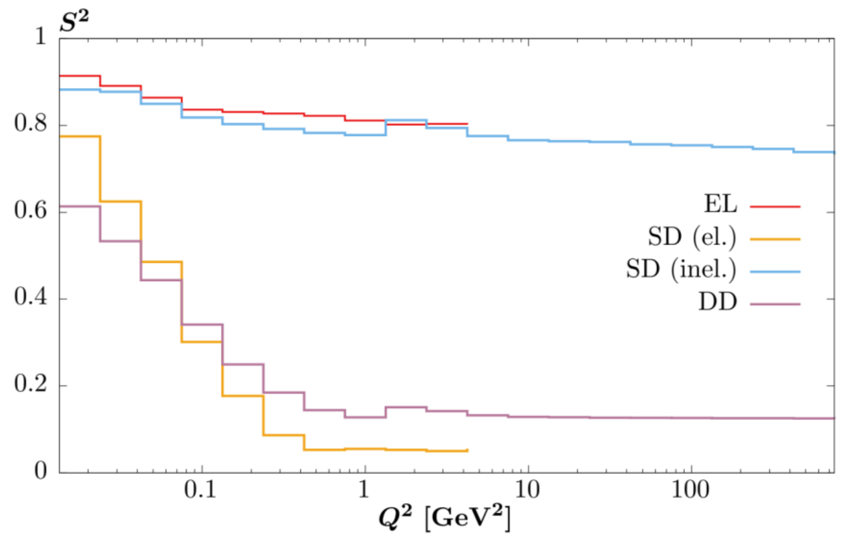

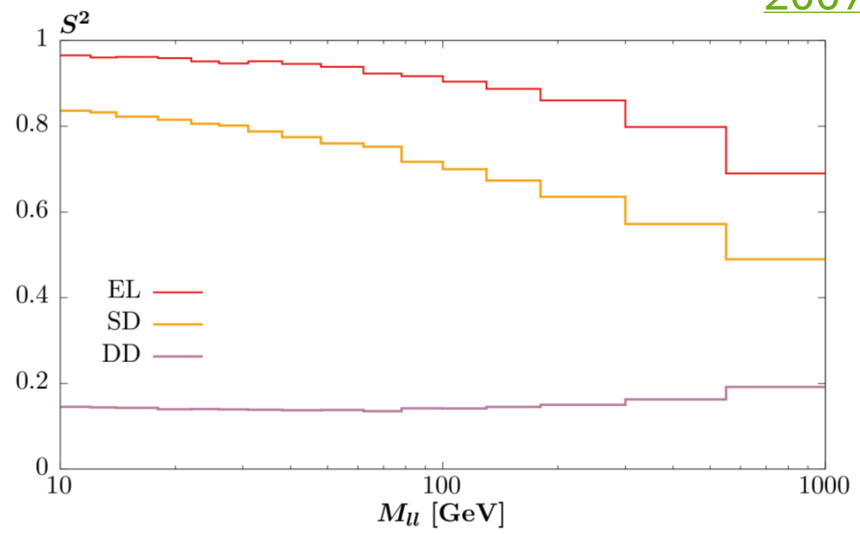

- **Reduces the cross section** of exclusive photon-induced processes

ATLAS Forward Proton (AFP) Spectrometer

- How do we measure the energy lost by protons which interact via photon exchange?
  - Protons are **scattered at small angles** (O(μrad)) proportional to their energy loss
  - Position **detectors far down the beamline** where transverse deflection is significant

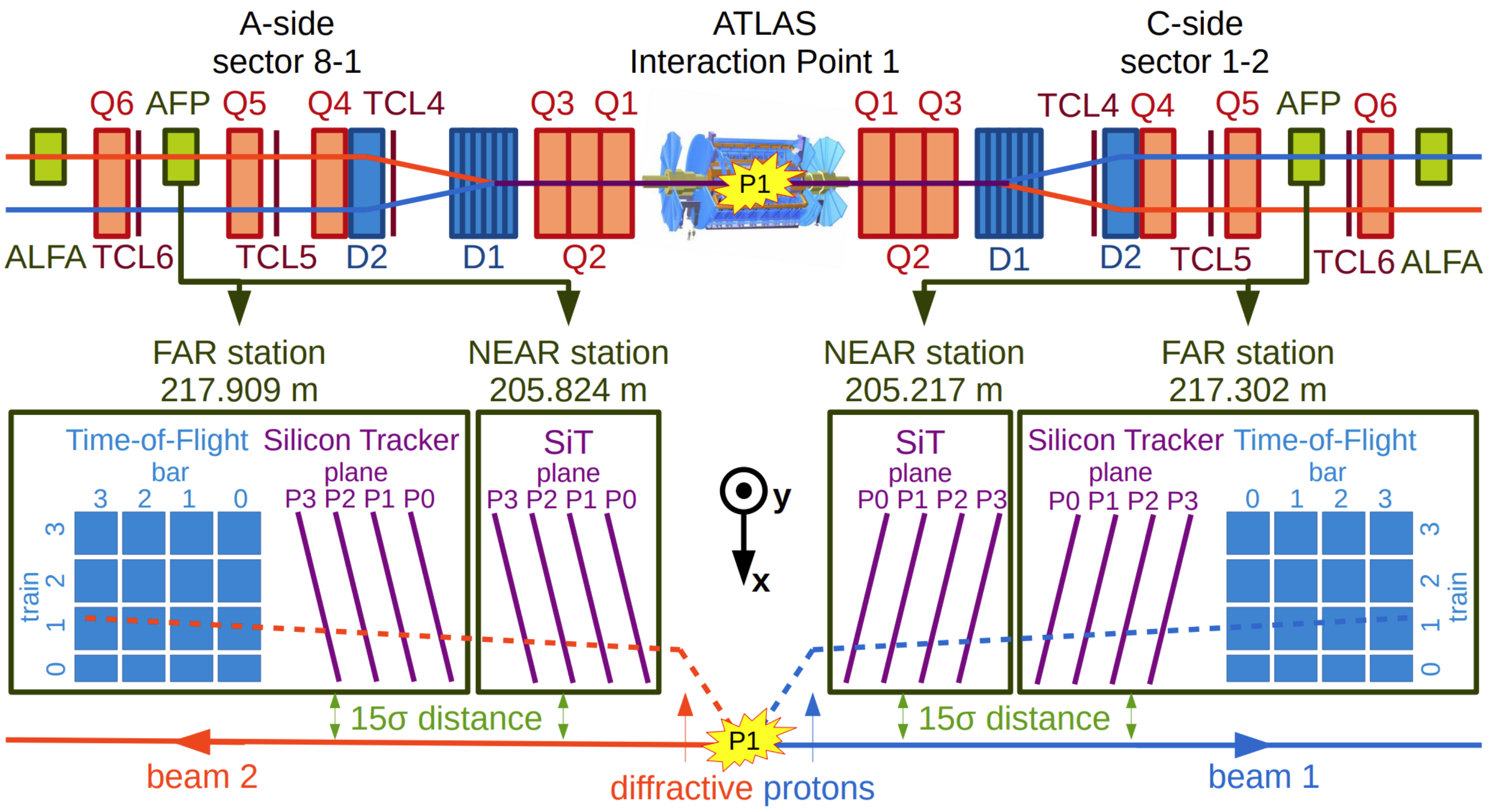

Proton fractional energy loss:

$$\xi = \frac{\Delta E_{\mathrm{proton}}}{E_{\mathrm{beam}}}$$

AFP

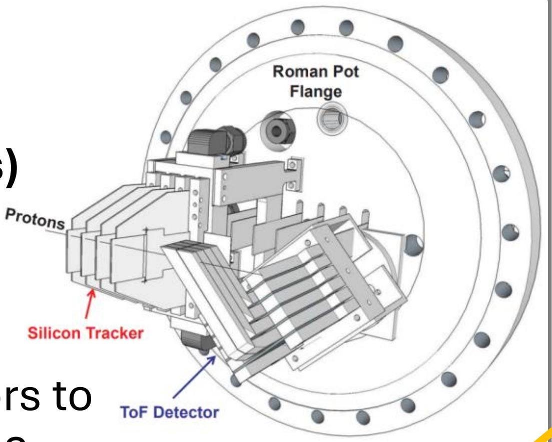

Roman Pots (RPs)

- Each station mounted on moveable RP
- Allows detectors to approach with 2 mm of the beam

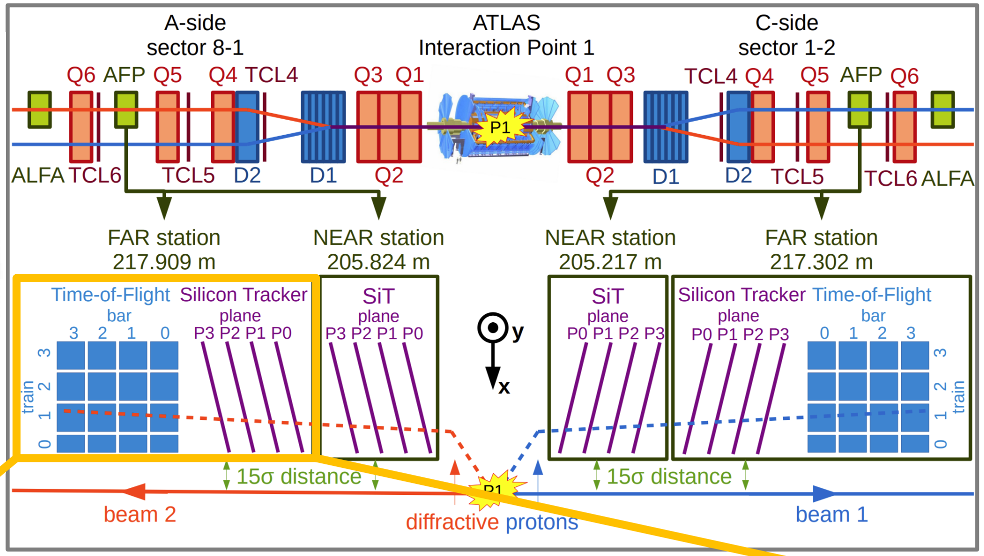

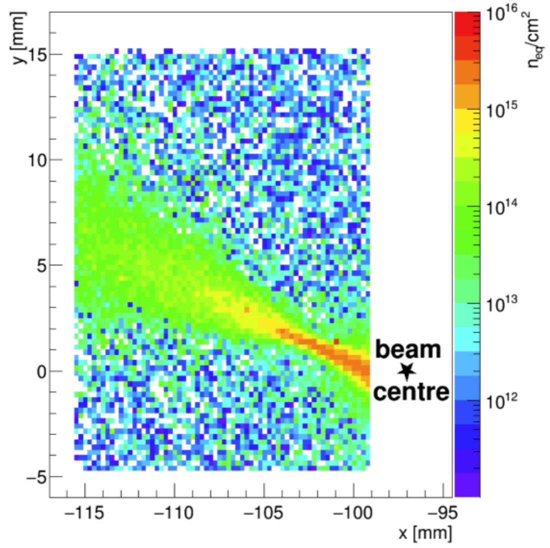

Time of Flight (ToF)

- Measure arrival time of protons at O(10) ps precision
  - ➢ Reconstruct vertex position at IP
- Cherenkov detector
- L-shaped light-guiding quartz bars
- 4 bars parallel to beam = train
- 4 trains per station
- Light collected by MCP-PMT for readout

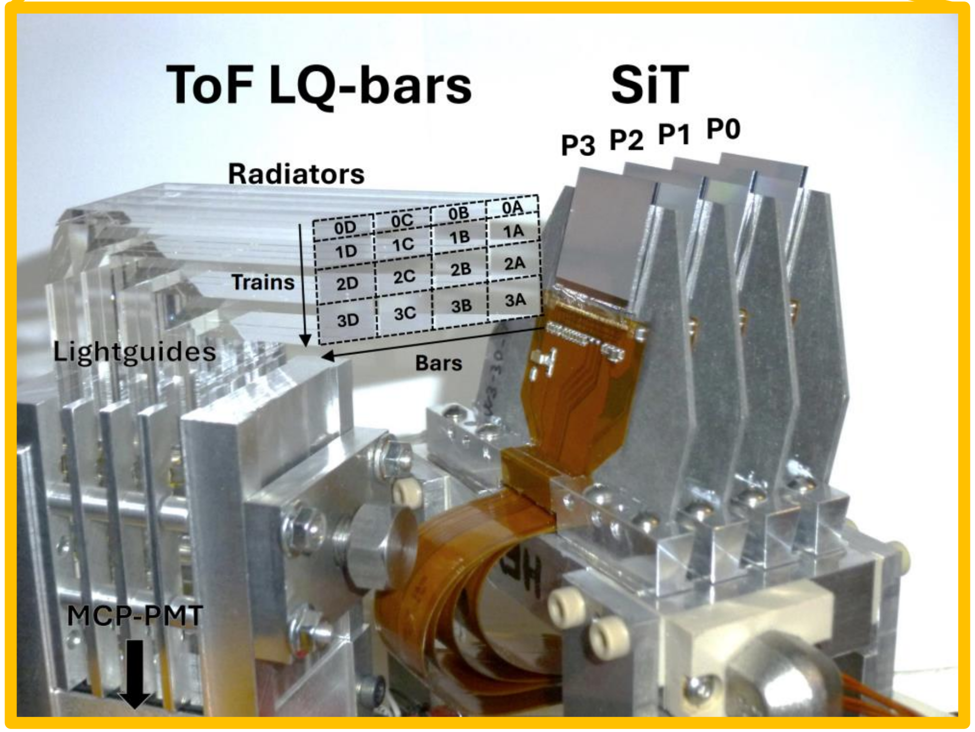

Silicon Trackers (SiT)

- Measure incident proton trajectories
- Two stations (NEAR and FAR) per side
- Four 3D silicon pixel sensors per station
- Need to withstand up to 3×10^{13} n_{eq}/cm^2 per fb^{-1} collected
- 336 × 80 pixels in x-y direction
- 50×250 μm^2 per pixel
- Tilted 14° about y axis to improve resolution

AFP Alignment

Measurement with AFP requires **precise alignment** of the detector components:

Local (Interplane) Alignment

- Alignment of the 4 sensor planes within a given SiT station
- Each plane has 6 d.o.f.:
- x and y translation and z rotation most important
- Iterative procedure performed on reconstructed tracks
- Calculate residual between track and cluster centres
  - ➢ Perform fit to minimise residuals
  - ➢ Repeat

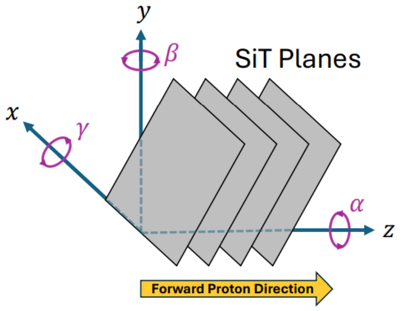

Global Alignment

- Alignment of the 4 AFP stations with the central ATLAS detector

$$x(s,t) = \boxed{x_{\text{pre-align}}} + \boxed{x_{\text{tracker}}} + \boxed{x_{\text{beam}}(s)} + \boxed{x_{\text{RP}}(s,t)} + \boxed{\delta x_{\text{corr}}(s)}$$

- Raw track position
- SiT module position
- Beam position – measured in special runs
- Roman pot position – distance of insertion
- In-situ correction – from analysis of dimuon events

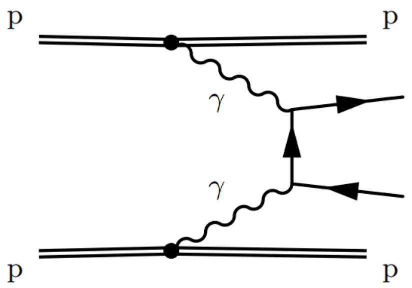

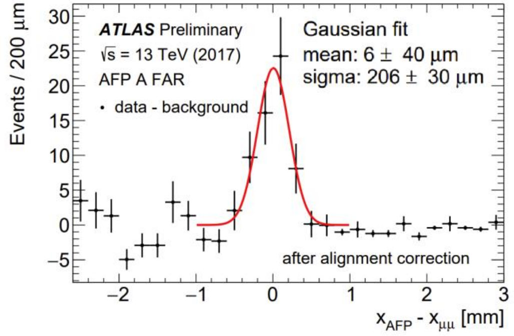

Forward Proton Reconstruction

SiT pixel hits → **SiT clusters** → **Tracks** → **Protons**

SiT pixel hits → SiT clusters

Coordinates: charge-weighted average of hits

Hits recursively combined with neighbours

Selection: only consider neighbours in x direction

Interplane alignment correction applied

SiT clusters → Tracks

Coordinates: linear regression of cluster positions

At least two clusters in SiT station combined

Selection: x-y separation of clusters < 0.5 mm

Global alignment correction applied

Tracks → Protons

Take NEAR station x and Δx slope between stations

Tracks in both NEAR and FAR stations combined

Selection: distance between tracks in x-y plane < 2 mm

Proton fractional energy loss:

$$\xi = \frac{\Delta E_{\text{proton}}}{E_{\text{beam}}}$$

Unique mapping between (x, Δx) and (p_x, ξ) of proton

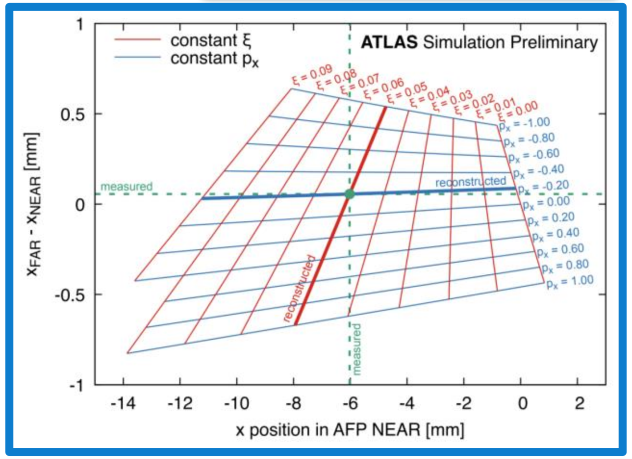

AFP acceptance: 0.02 < ξ < 0.12

Analysis Motivation

- **Forward proton measurements** from AFP allow calculation of **full four-momentum** of the central interaction in elastic photon-exchange processes
- Compare to **central system** measured by ATLAS to determine **what's missing**
  - ➢ Could reveal **BSM particles** not detectable by ATLAS e.g. dark matter, SUSY, etc.
- Perform search for **missing mass X** produced alongside **visible boson-like V** decaying to leptons
  - ➢ Reconstruct mass of X and perform **search for narrow resonance**

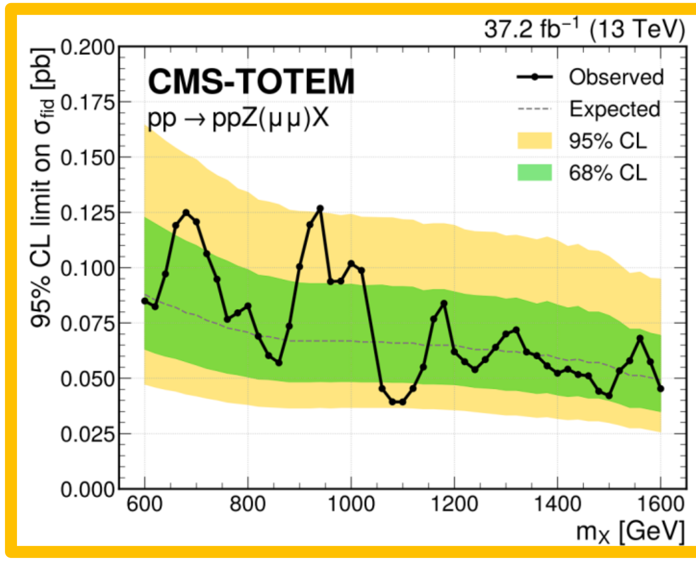

- Equivalent analysis published by CMS
- No significant excess observed, limits set on signal cross section

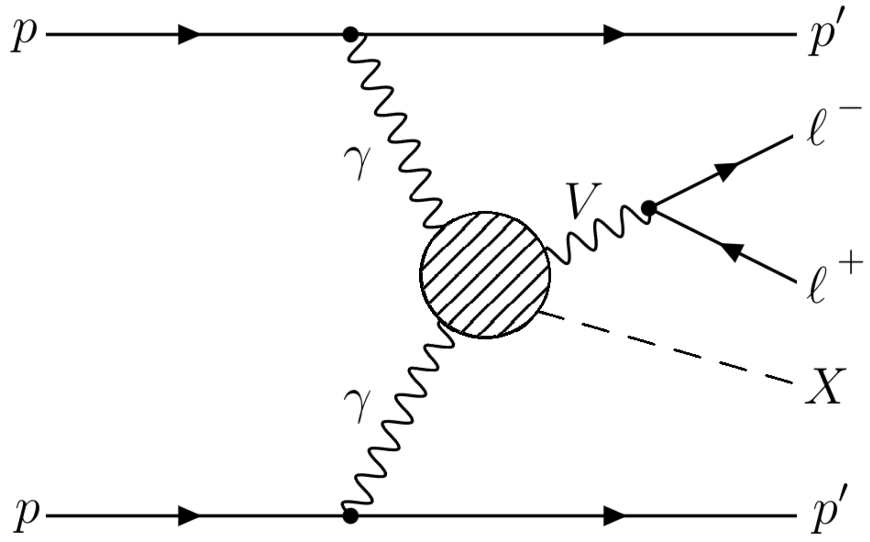

Missing Mass Method

The missing mass present in each event is calculated as:

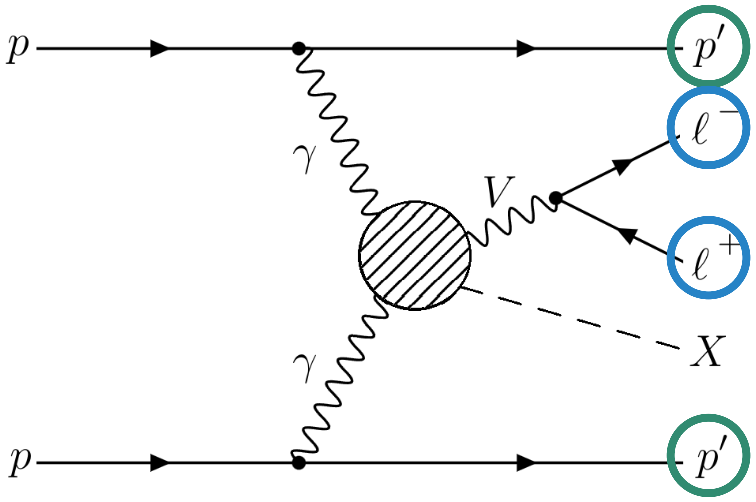

$$m_X^2 = (E_{\gamma\gamma} - E_{\ell\ell})^2 - (\overrightarrow{p_{\gamma\gamma}} - \overrightarrow{p_{\ell\ell}})^2$$

$$= \left[\begin{pmatrix} \Delta E_{p_A} + \Delta E_{p_C} \\ 0 \\ 0 \\ \Delta E_{p_A} - \Delta E_{p_C} \end{pmatrix} - \begin{pmatrix} E_{\ell\ell} \\ p_x^{\ell\ell} \\ p_y^{\ell\ell} \\ p_z^{\ell\ell} \end{pmatrix} \right]^2$$

AFP **ATLAS**

Improves over ATLAS missing **transverse** energy as it includes the **longitudinal** component

where ΔE_{p_A} and ΔE_{p_C} are the energy losses of the protons detected on AFP sides A and C respectively and we assume that the transverse momenta of the photons is negligible.

Resolution measured to be ~50 GeV across the measured range

Signal Simulation

Comparison between two generators using very different assumptions on underlying processes:

- Standalone **SuperChic** and **MadGraph** within Athena

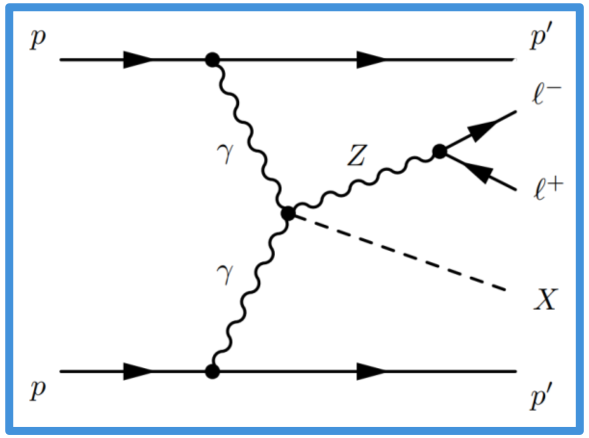

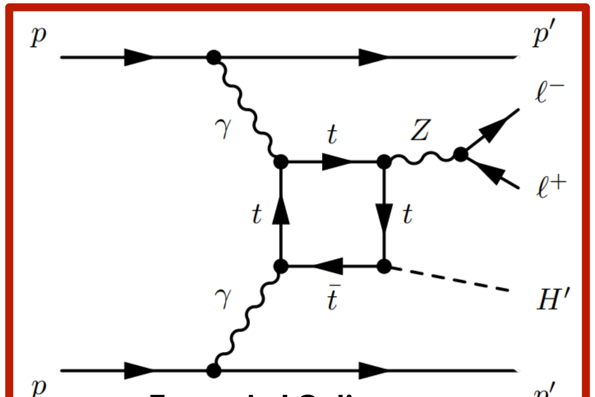

Example LO diagram

SuperChic (Simple dedicated generator):
New process implemented, simple direct simulation

MadGraph (ALP production):
Testing axion-like particle process with two ALPs: One long-lived (X) and the other (V) decaying to leptons

MadGraph (Higgs derivation):
Custom Higgs mass, forced to not decay to mimic our X particle

SuperChic: $300 \leq m_X \leq 900$ GeV
MG ALP: $200 \leq m_X \leq 800$ GeV
MG ZH: $100 \leq m_X \leq 800$ GeV
ℓ = electron or muon

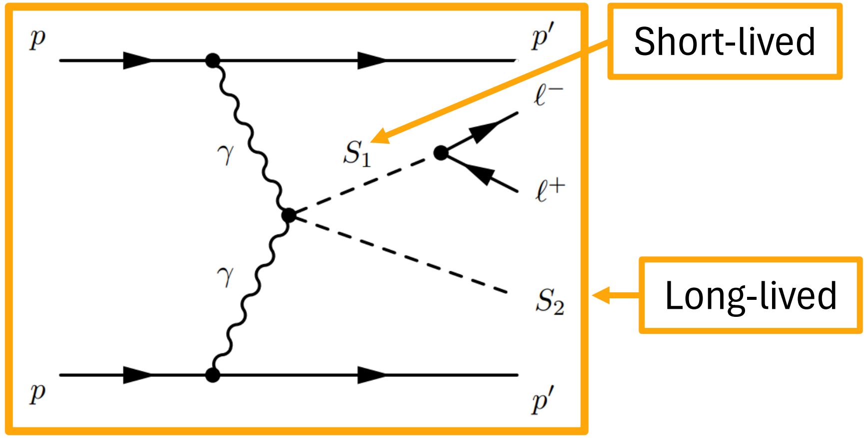

Setting limits on each model separately

Signal Kinematic Comparison

- **Kinematic comparison** between signal models with m_X = 500 GeV at **generator level**:

Dilepton p_T

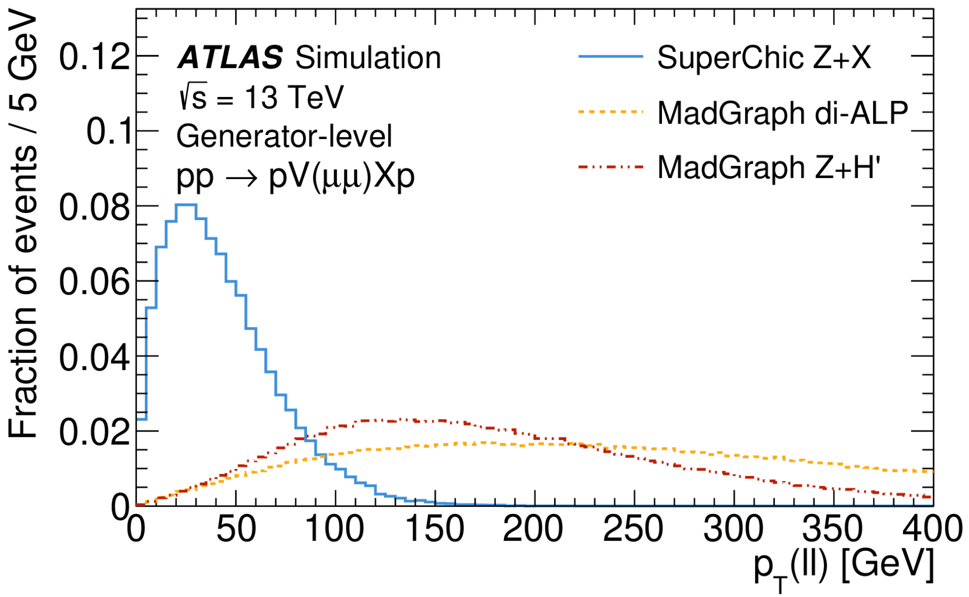

Proton ξ

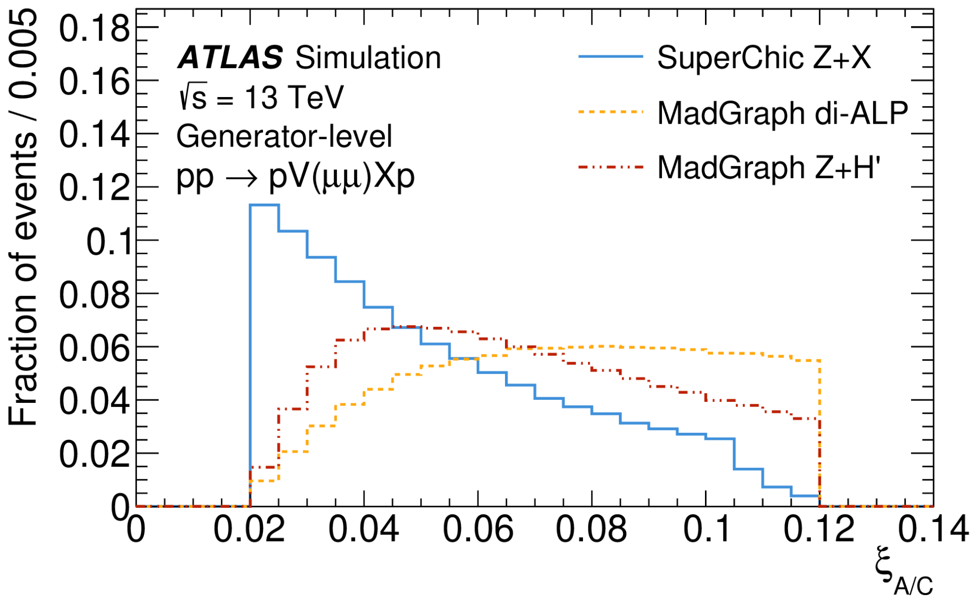

- MadGraph models have **significantly higher dilepton p_T**
  - Balanced by higher skew of proton ξ distribution
- Dilepton and missing mass distributions well matched with equivalent widths

Wide range of phase space covered by the three models

Data

- **Only 2017 data** available for AFP in Run 2
  - In 2015, AFP was not yet operational
  - In 2016, AFP was inserted only on side C
  - In 2018, data was recorded with AFP but was incorrectly synchronised with ATLAS
- 46.9 fb^{-1} recorded by ATLAS in 2017:

46.9 fb^{-1} → 32.0 fb^{-1} → 26.0 fb^{-1} → 19.2 fb^{-1} → 14.7 fb^{-1}

AFP insertion | ATLAS GRL | AFP GRL | Remove low efficiency runs

- Loosest available unprescaled single and dilepton triggers applied

AFP GRL:

- All stations inserted to nominal data-taking positions
- At least two SiT planes in each station have high voltage on
- Data Acquisition system is fully functional

Pre-Selection

Define **pre-selection** to create sample for data-driven background modelling and studies during the analysis:

- Require at least two same-flavour, opposite sign leptons (e^+e^- or $\mu^+\mu^-$)
- Require **exactly one** proton per side

< 1 proton on at least 1 side

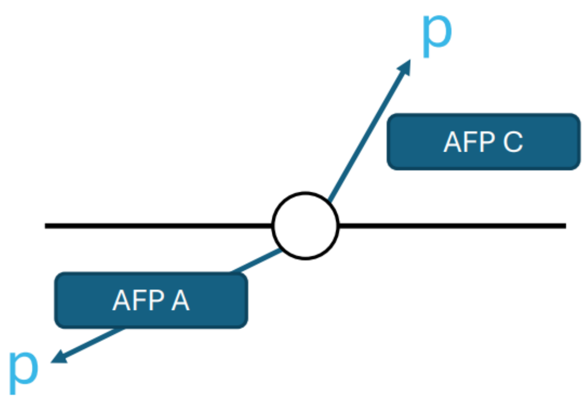

Cannot reconstruct missing mass without protons on both sides

Exactly 1 proton on both sides

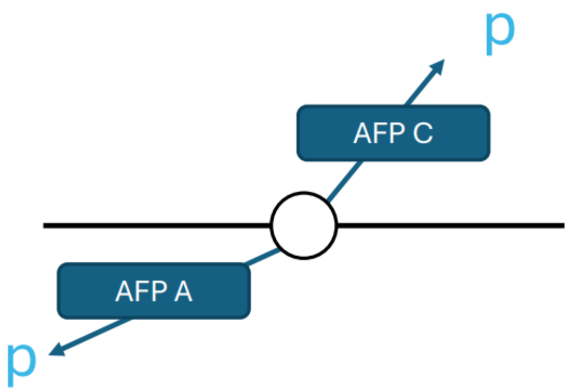

Reconstruct missing mass using one proton per side (assuming they are the correct protons)

> 1 proton on at least 1 side

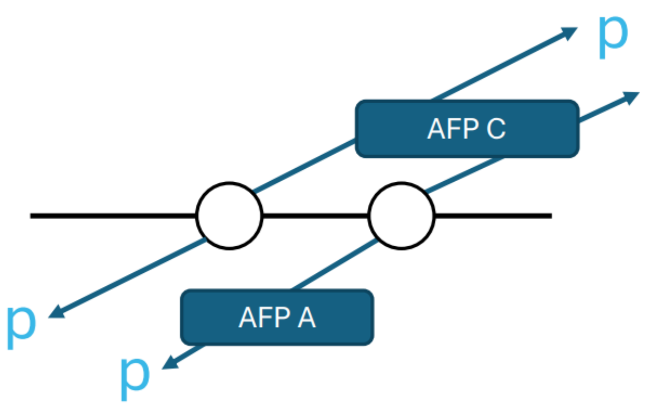

No way to select between multiple protons on the same side

Signal Selection

Define **signal selection** to optimise signal-to-background ratio and use for final fits:

Feature	Signal Region Criterion
Electrons	
Kinematic	$p_T > 18$ GeV
Identification	LooseAndBLayer
Muons	
Kinematic	$p_T > 15$ GeV
Identification	Medium
Dilepton	
Charge	$q_{\ell_1} + q_{\ell_2} = 0$
Kinematic	$p_T > 20$ GeV
Mass	$m_{\ell\ell} > 50$ GeV
Track number	$N^{0.5\text{ mm}}_{p_T > 500\text{ MeV}} = 0$
Protons	
Kinematic	$0.035 < \xi < 0.08$ NEAR station track $x < -3.5$ mm
Number of stations	Double only

Loose lepton requirements to maximise statistics

Impose loose dilepton mass cut to remove quarkonia and dilepton p_T cut to remove background

Track veto (in a few slides)

Tight proton ξ requirement corresponds to region where efficiency is well understood

Fiducial Selection

Define **fiducial selection** similar to signal selection

- Applied at **generator-level** to simulated signal samples
- Reduces search phase space to the one which our detectors are sensitive to

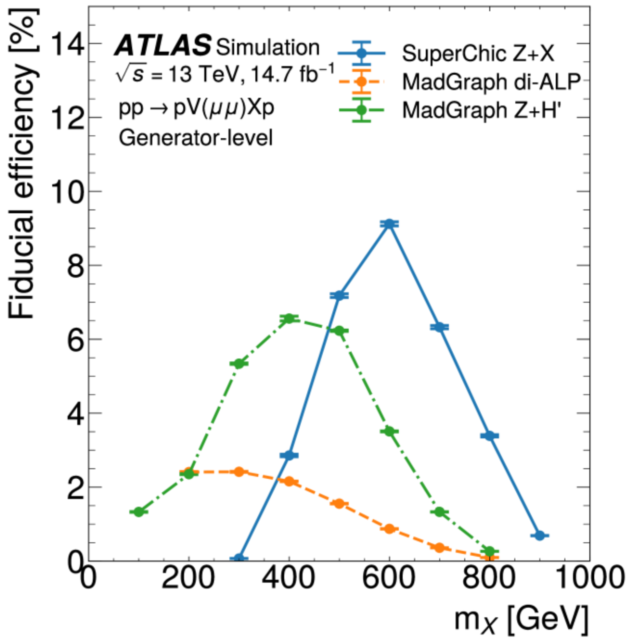

Fiducial selection efficiency for each signal model and mass

Feature	Criterion
Electrons	$p_T > 18$ GeV $\lvert\eta\rvert < 2.47$
Muons	$p_T > 15$ GeV $\lvert\eta\rvert < 2.4$
Dilepton system	Same flavour, opposite charge $m_{\ell\ell} > 50$ GeV $p_T^{\ell\ell} > 20$ GeV
Protons	$0.035 < \xi < 0.08$

Generator level ξ cut greatly reduces background from incorrectly selected protons (more in a few slides)

- Events falling outside fiducial selection considered as **additional background component**

Track Veto

High track density resulting from multiple overlapping interactions

Require a **clear window** (no other tracks) around dilepton vertex

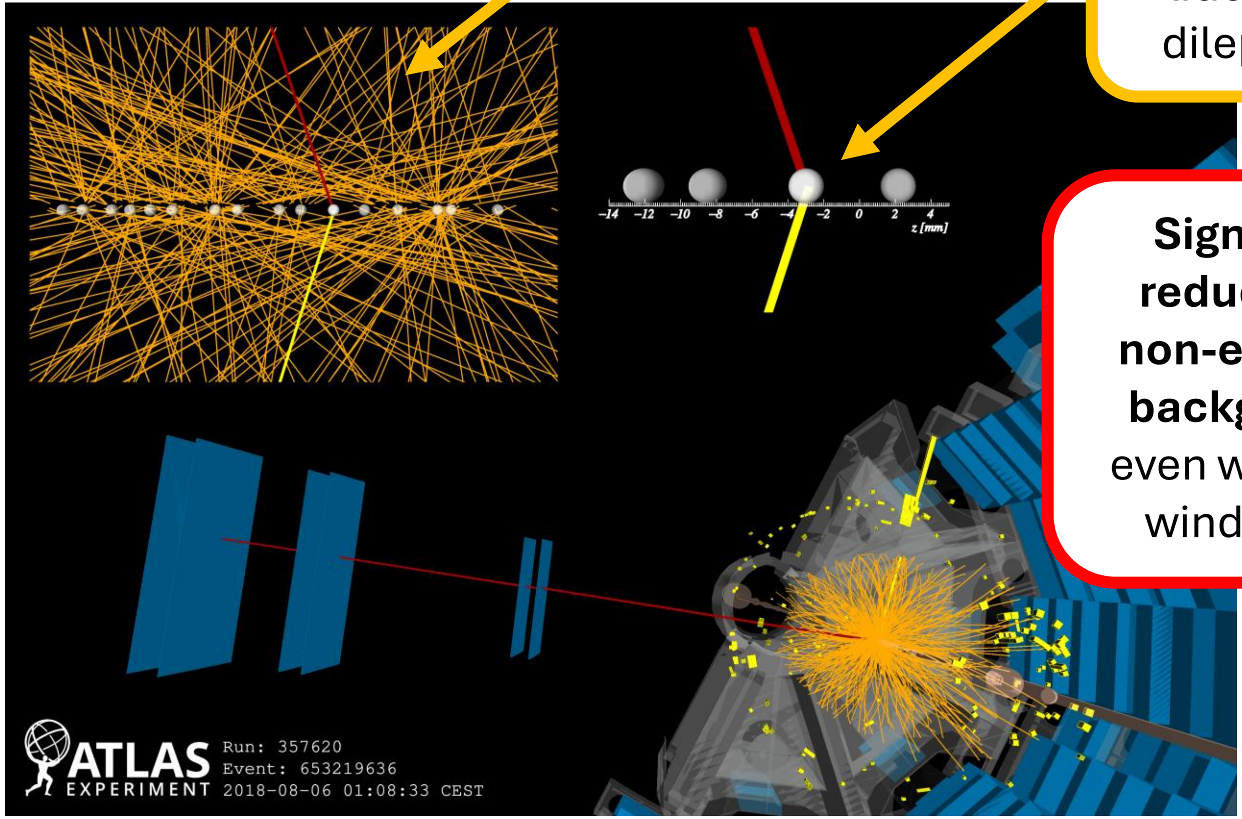

Significant reduction in non-exclusive backgrounds even with small window size

Distance of the closest additional inner detector track to the dilepton vertex

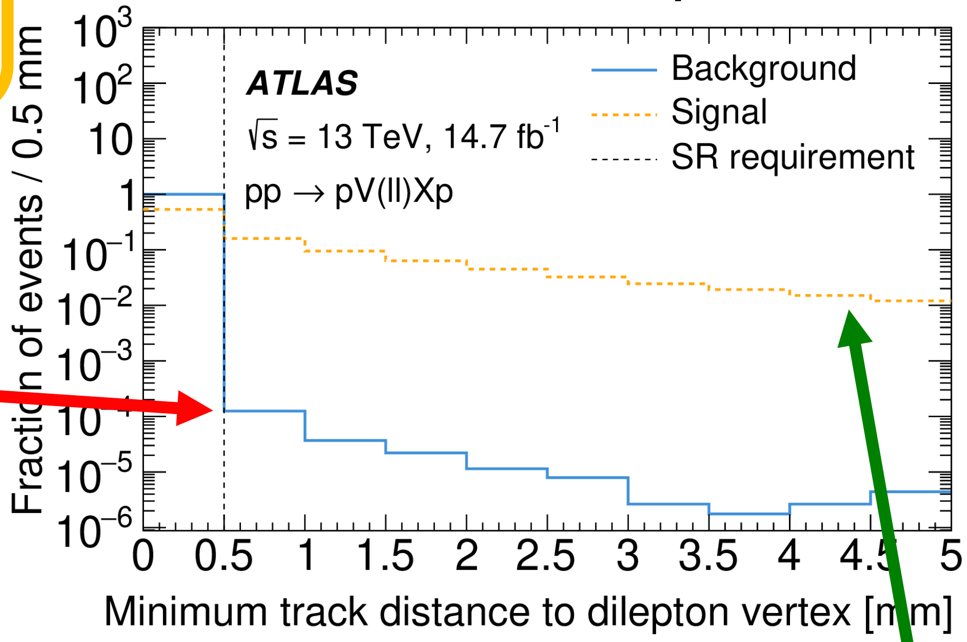

Signal efficiency much higher due to no additional event components – only loss is due to **random intercept** by tracks from pile-up interactions

Low-p_T Tracks

Standard **“high-p_T”** ATLAS tracks have **p_T > 500 MeV**

- Many background processes have soft tracks below this threshold
- Including **“low-p_T” tracks** could greatly enhance the power of the track veto

New technique now available for track reconstruction down to **p_T > 100 MeV** (described in ATL-COM-PHYS-2024-270)

- Computationally expensive and slow process
- Performed on filtered sample with maximum of 15 high-p_T tracks within track veto window

Projection:

- Up to 5 times improvement in background rejection
- Only 20% additional loss of signal
- Up to 2 times improvement in sensitivity

Reality:

- Extremely low statistics in data and signal samples
- Unstable fitting requiring increased bin widths
- Degraded any potential improvement ☹

Low-p_T Tracks

Standard "**high-p_T**" ATLAS tracks have **p_T > 500 MeV**

- Many background processes have soft tracks below this threshold
- Including "**low-** ... ck veto

New technique n ... **MeV** (described in ATL-COM-PHYS-2 ...

- Computationa ...
- Performed on f ... in track veto window

Projection:

- Up to 5 times im ... background reje...
- Only 20% additional loss of signal
- Up to 2 times improvement in sensitivity

... stics in data and ...

- Unstable fitting requiring increased bin widths
- Degraded any potential improvement ☹

Huge potential for a future analysis with a larger dataset!

Background Modelling

Dominant background in **combinatorial background**

- Central dilepton systems from SM processes wrongly combined with unassociated protons from independent pile-up interactions

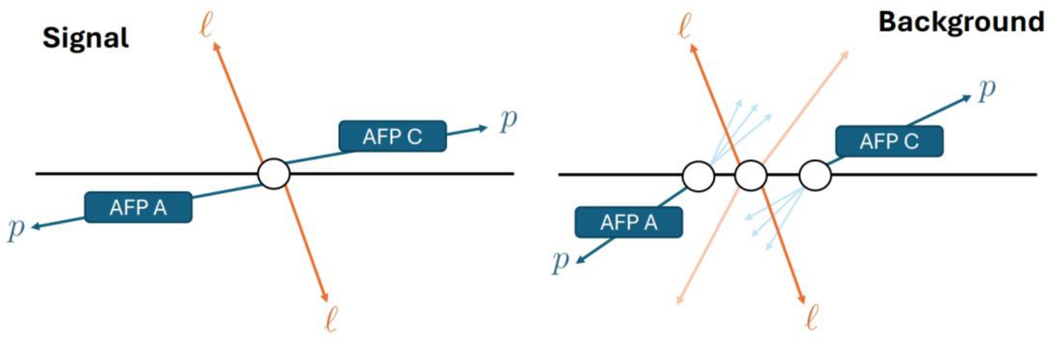

Central dileptons come from several **SM processes**:

- Z+jets
- Top quark production: Wt and ttbar
- Diboson production: WW, WZ and ZZ
- Photon-induced dilepton production: ll and WW
- Misidentified (fake) leptons

Protons originate mainly in **single-diffractive** (QCD Pomeron exchange) processes between **pile-up protons**

Modelled using **data-driven event mixing** procedure:

- No simulation required
- No scale factors or corrections
- Only systematics come from normalisation and statistical uncertainty

Event Mixing

- Primary background in AFP analyses is combinatorial
  - Formed by incorrect combination of protons with uncorrelated central interaction
- Easily and accurately modelled using data-driven approach **event-mixing:**

1. Select even shift **i** between 1 and N-1 (N = sample size)
2. Separate central and proton component of each event
3. Shift central components by **i** positions along the dataset
4. Recombine shifted event components

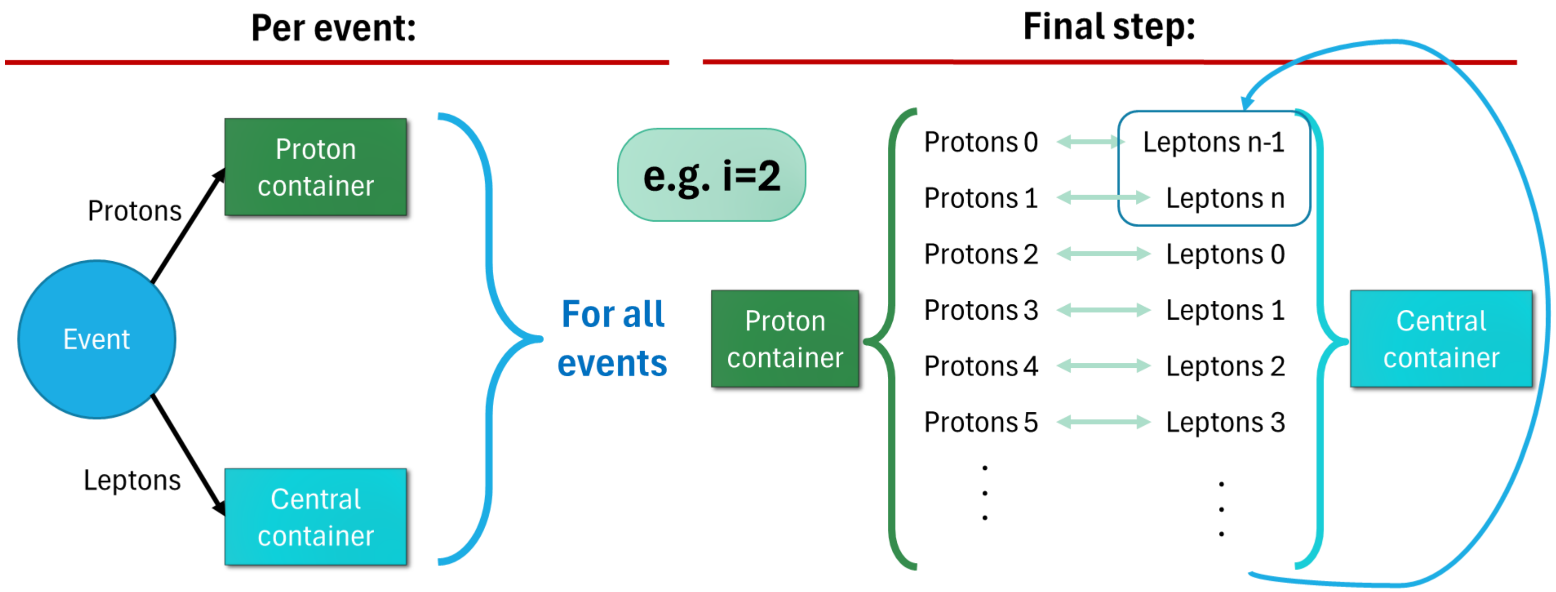

Mixed event components are uncorrelated as in background

Background Modelling

Dominant background in **combinatorial background**

- Central dilepton systems from SM processes wrongly combined with unassociated protons from independent pile-up interactions

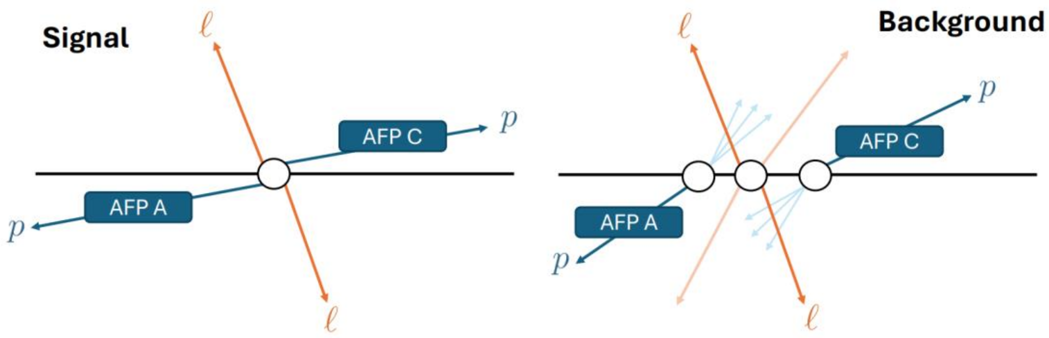

Central dileptons come from several **SM processes**:

- Z+jets
- Top quark production: Wt and ttbar
- Diboson production: WW, WZ and ZZ
- Photon-induced dilepton production: ll and WW
- Misidentified (fake) leptons

Protons originate mainly in **single-diffractive** (QCD Pomeron exchange) processes between **pile-up protons**

Modelled using **data-driven event mixing** procedure:

- No simulation required
- No scale factors or corrections
- Only systematics come from normalisation and statistical uncertainty

Can **average over several mixed samples** with different event-shifts to create **high statistics** background model

We use $2 \leq i \leq 101$ **~1% uncertainty**

Background Validation with MC

Create secondary background model using MC simulation to validate data-driven model

- Simulate central SM processes
- Overlay database of randomly assigned pile-up protons taken from 2017 data
- Model fake lepton contribution using same-sign lepton selection on data

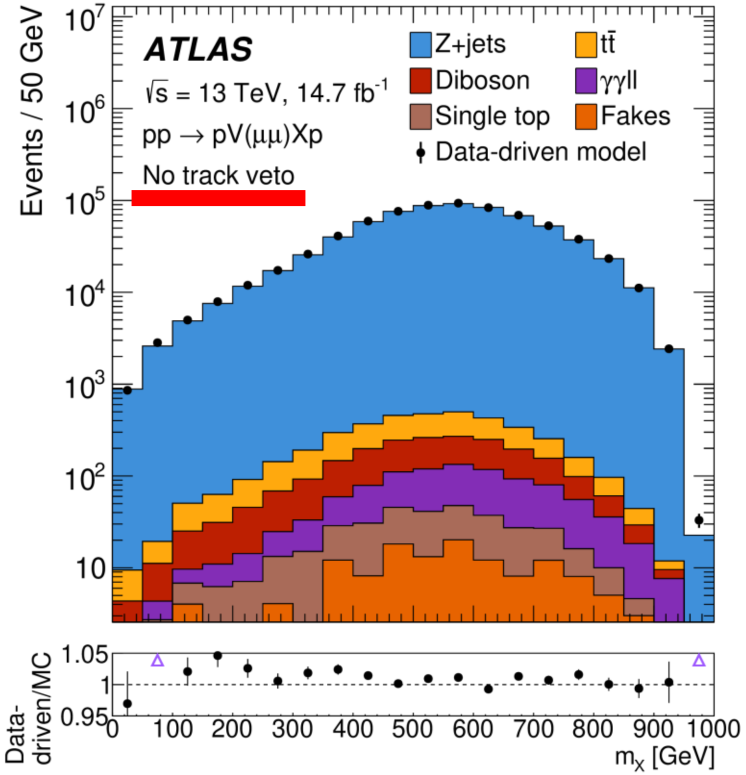

Excellent agreement observed
Data-driven model validated for use in final fits

Distributions after track veto are normalised due to known mismodelling of underlying event
Still good agreement

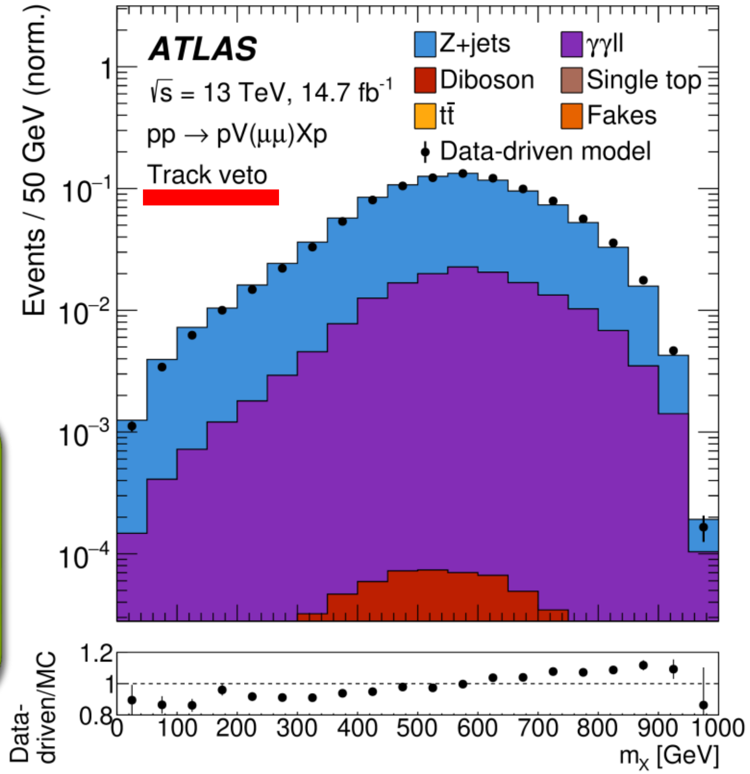

Signal-Induced Background

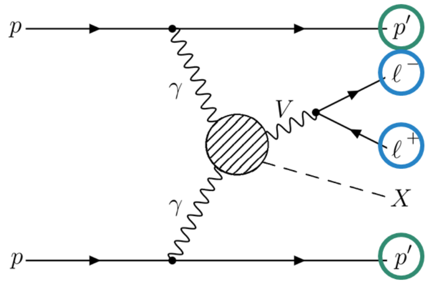

$$m_X^2 = (E_{\gamma\gamma} - E_{\ell\ell})^2 - (\overrightarrow{p_{\gamma\gamma}} - \overrightarrow{p_{\ell\ell}})^2 = \left[\underbrace{\begin{pmatrix} \Delta E_{p_A} + \Delta E_{p_C} \\ 0 \\ 0 \\ \Delta E_{p_A} - \Delta E_{p_C} \end{pmatrix}}_{\text{AFP}} - \underbrace{\begin{pmatrix} E_{\ell\ell} \\ p_x^{\ell\ell} \\ p_y^{\ell\ell} \\ p_z^{\ell\ell} \end{pmatrix}}_{\text{ATLAS}} \right]^2$$

- Significant amount of **pile-up protons** detected in AFP
- Signal protons can go undetected due to being **outside AFP acceptance** or detector inefficiency
- Pile-up proton detected in its place will be accepted by the selection as a signal proton

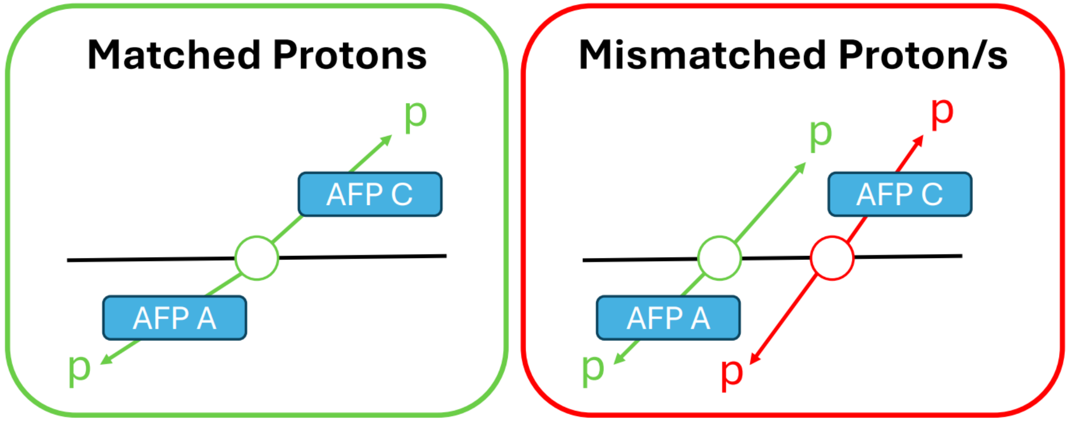

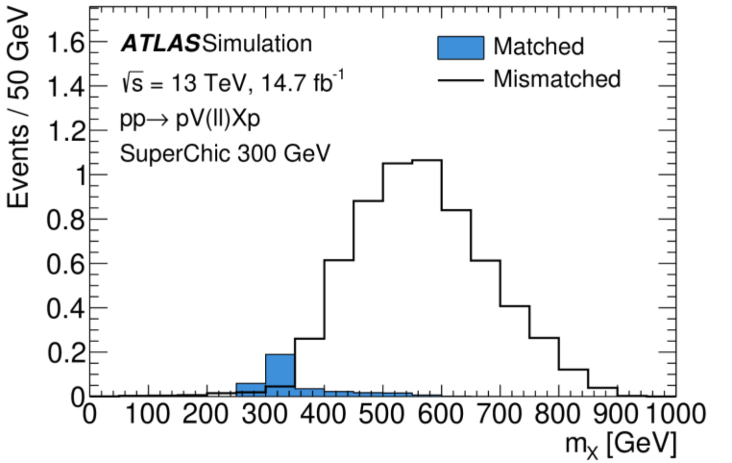

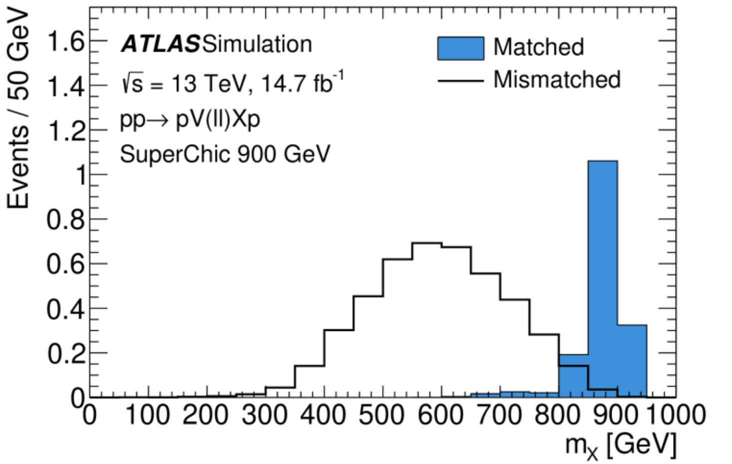

- Causes inaccurate reconstruction leading to significant smearing of the signal peak in the model (**values away from signal peak**):
- Effect becomes large at extreme values of m_X, especially high values
  - More likely for signal protons to fall outside AFP acceptance

Dominantly occurs for events **outside the fiducial selection**
These events are included as an **additional background component**

Systematics

Dominant systematic uncertainties arise from track veto and AFP in signal simulation:

Uncertainty on signal efficiency of track veto

Taken from difference between estimates obtained using two different methods

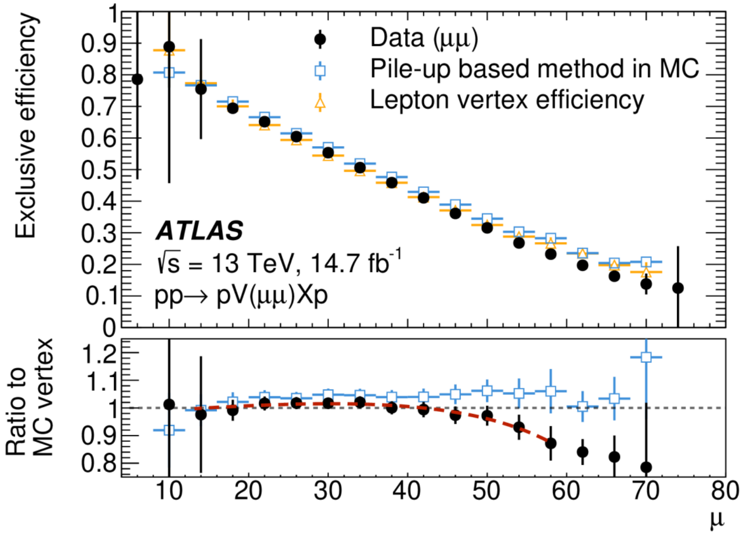

Uncertainties in AFP simulation

Proton transport: Modifies beam slope by ±50 μrad

Global alignment: Modifies global alignment of AFP stations by ±300 μm in x

Smearing: Modifies width of distribution used to smear truth-level proton data by ±0.05 mm

Large variation in dominant proton systematics across signal mass range e.g. proton transport:

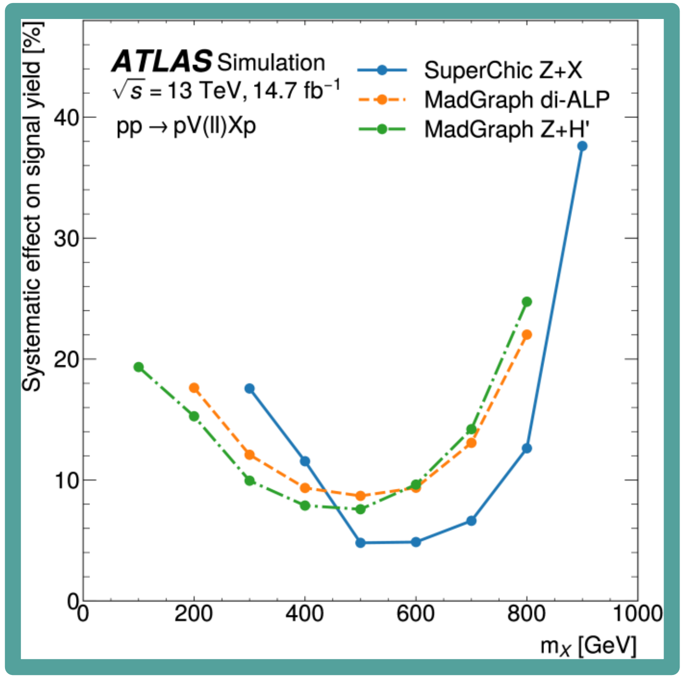

Systematics – Soft-Survival

Estimated effect of soft-survival on signal yield using photon-induced dilepton events simulated in SuperChic

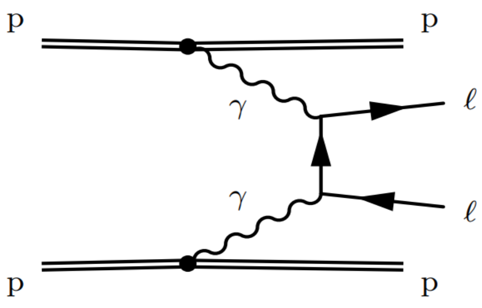

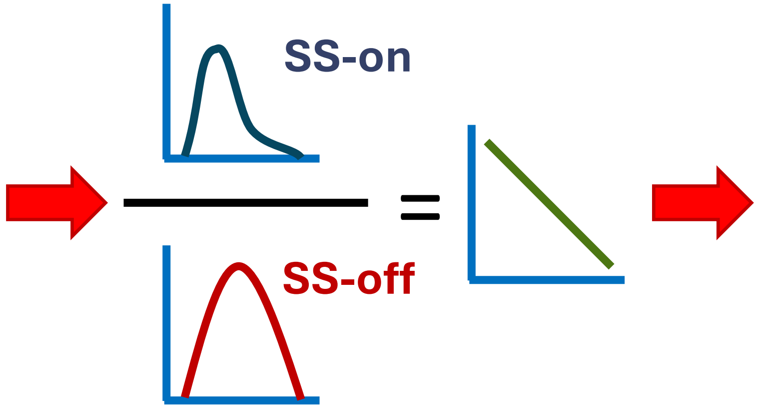

- Ratio fitted to linear parametrisation

$$S = 0.9387 - 0.000365\, m_{sys}$$

- Applied event-by-event to signal

- Only considered for the SuperChic models since the generator implements this effect
- Scale factor applied as systematic variation for MadGraph models

Systematic for SuperChic taken from studies of dilepton exclusive production

(arXiv:1708.04053, arXiv:2009.14537)

Uncertainty	Effect on event yield		
	Signal		
Signal model	SUPERCHIC	MADGRAPH di-ALP	MADGRAPH $Z + H'$
Soft survival factor	20.0%	20.0%–38.7%	20.0%–38.7%

Statistical Analysis

- Originally used 50 GeV bins across full $0 \leq m_X \leq 1000$ GeV range
  - Due to low data and signal model statistics in signal region, switched to **single bin** approach using **mass window** around hypothesised signal mass:

Signal mass [GeV]	Signal region [GeV]
100	0–300
200	100–300
300	200–400
400	300–500
500	400–600
600	500–700
700	600–800
800	700–900
900	700–1000

- ✓ Removed fit stability issues
- ✓ Mass window reduced signal-induced background to negligible levels
- ✗ Reduction in sensitivity (up to factor of 2)
- ✗ Wider bins required at tail masses

Control Regions

- Data-driven background model normalised with respect to a **control region**, to avoid bias from **potential signal contamination** in the data:
  - Defined as m_X range outside the **signal mass window** for each signal model
  - **~100 GeV gap** imposed on either side for most mass points to ensure no signal contamination
  - Control region range extended for low signal mass due to low statistics

Signal mass [GeV]	Signal region [GeV]	Control region(s) [GeV]
100	0–300	300–400
200	100–300	300–400
300	200–400	0–100, 400–450
400	300–500	600–1000
500	400–600	700–1000
600	500–700	400–450, 800–1000
700	600–800	450–500, 900–1000
800	700–900	400–600
900	700–1000	400–600

Simultaneous fit performed across signal and control regions

- Approach verified using **signal injection tests**
  - Signal injected into data had **no effect** on resulting background normalisation

Results

Perform **likelihood fit** between observed data and signal + background model

- Simple fits due to single-binned approach

Pre and post fit distributions for each signal model and mass:

- Pre-fit signals are normalised to 50 fb for reference

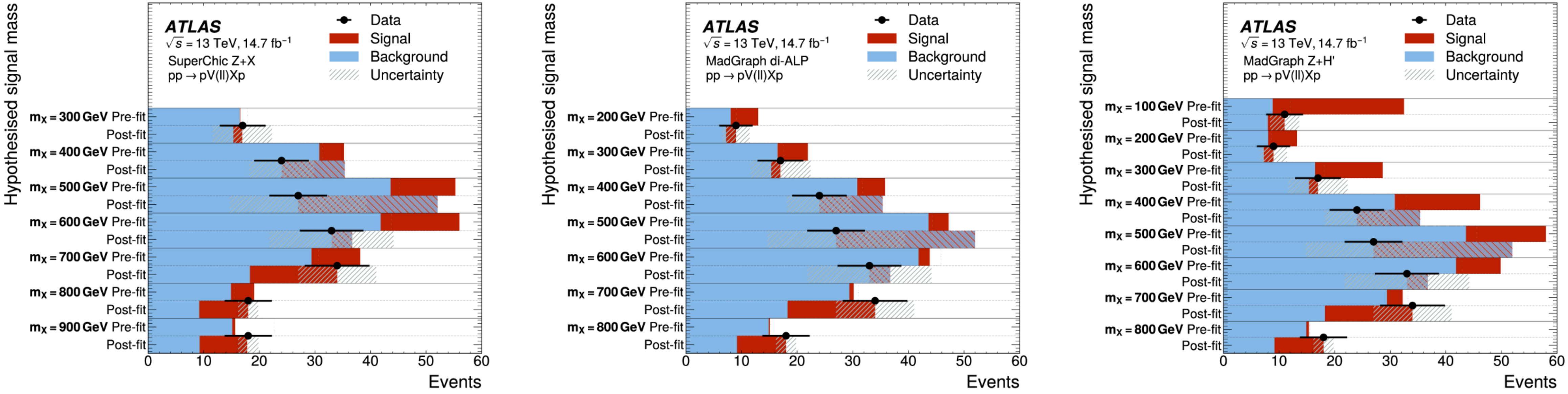

Equal number of cases with excess and lack of observed data compared to background prediction – no significant signal observed

Results – Signal Cross Section Upper Limits

No significant deviations from SM so upper limits are set at 95% CL on the **signal fiducial cross section** for each model with CL_s method

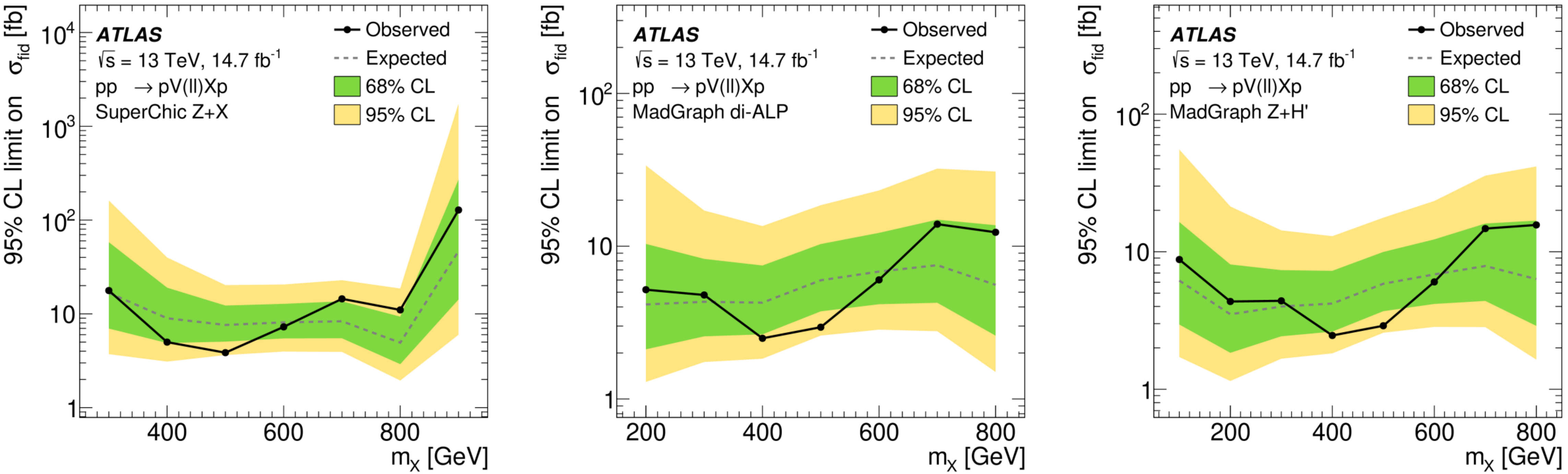

Very similar limits around O(10) fb obtained for each model despite significant difference in kinematics

Results – CMS Comparison

Compare to limits from similar CMS analysis

- CMS have **larger dataset** (37.2 fb^{-1} vs 14.6 fb^{-1})
- CMS CT-PPS detector has much higher upper limit on proton ξ than AFP (0.20 vs 0.12)
  - **Much higher missing mass limit ~1.6 TeV**

- Use **SuperChic Z+X model** – designed to be equivalent to the CMS model
- Scale ATLAS limits **to CMS's fiducial region**
- Compare results with **no soft-survival** included

- **Improvement** in sensitivity observed for several common mass points
  - Mainly thanks to **track veto selection**
- Limits obtained at **lower signal masses**

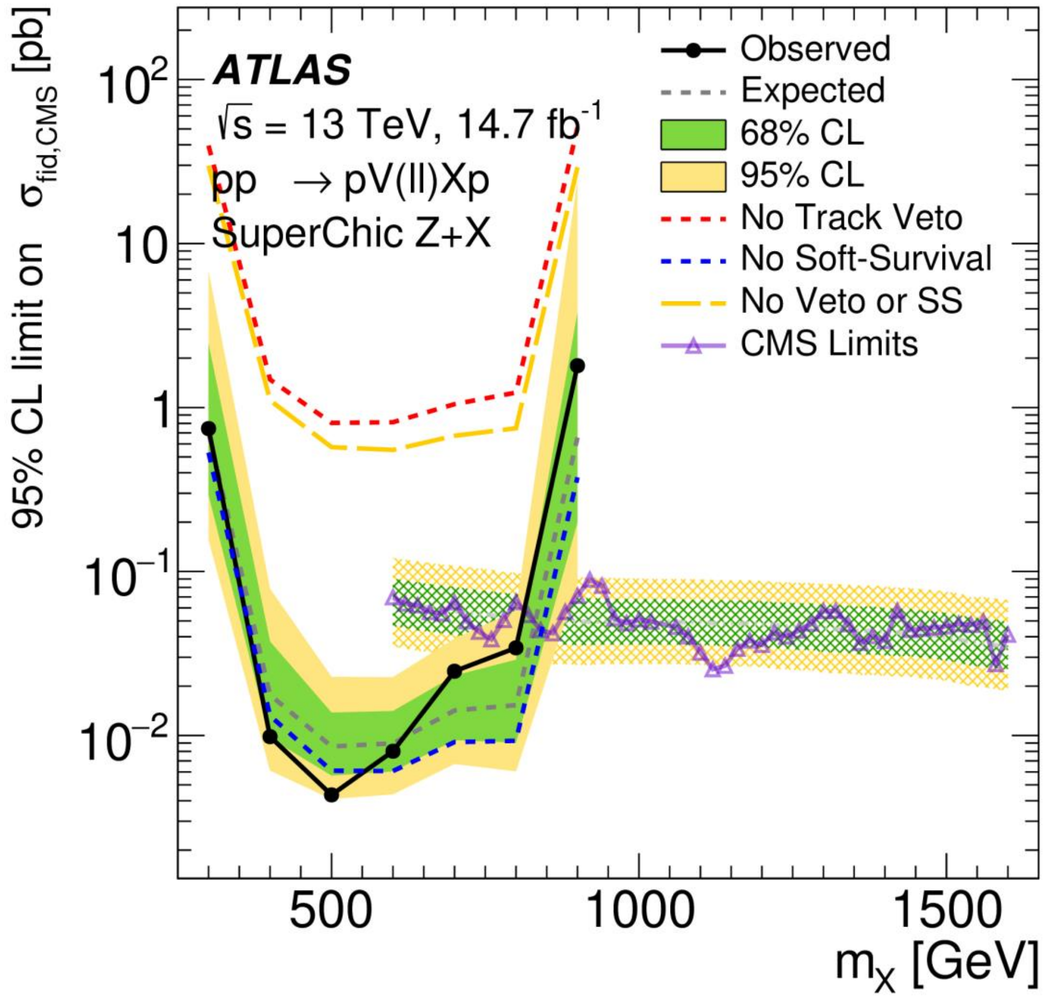

Results – Model Independent Limits

Additionally obtained **model-independent** upper limits at 95% CL on the **visible cross-section**

- Visible cross-section = cross-section × acceptance × efficiency for **BSM processes**
- **Generic signal model** used with 50 GeV width in single-bin fits
- Limits obtained both **with and without the track veto applied**, to allow for non-exclusive signals

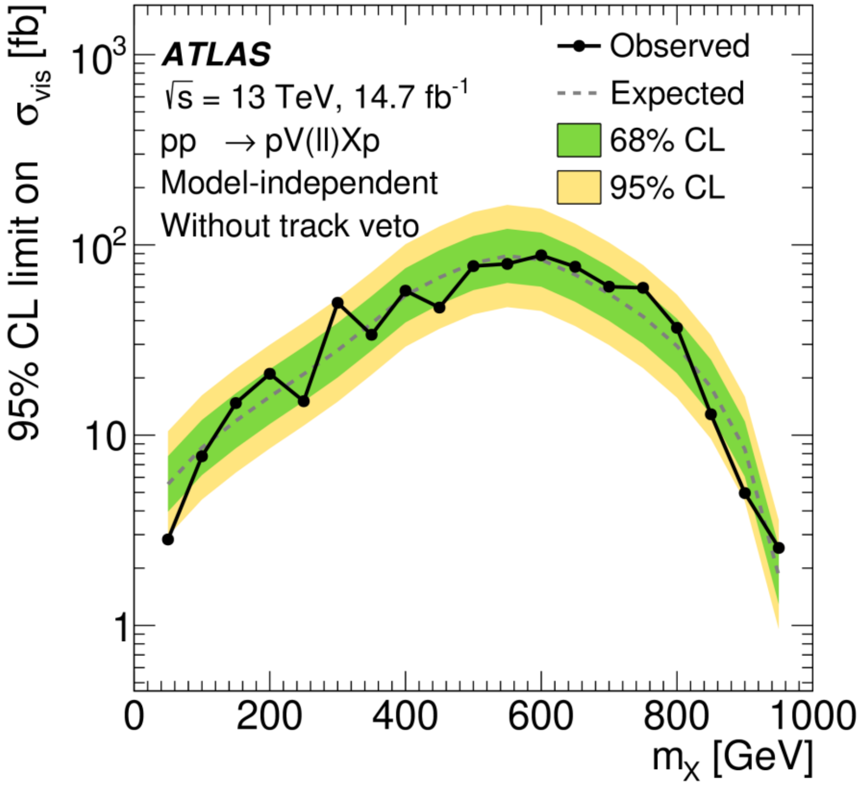

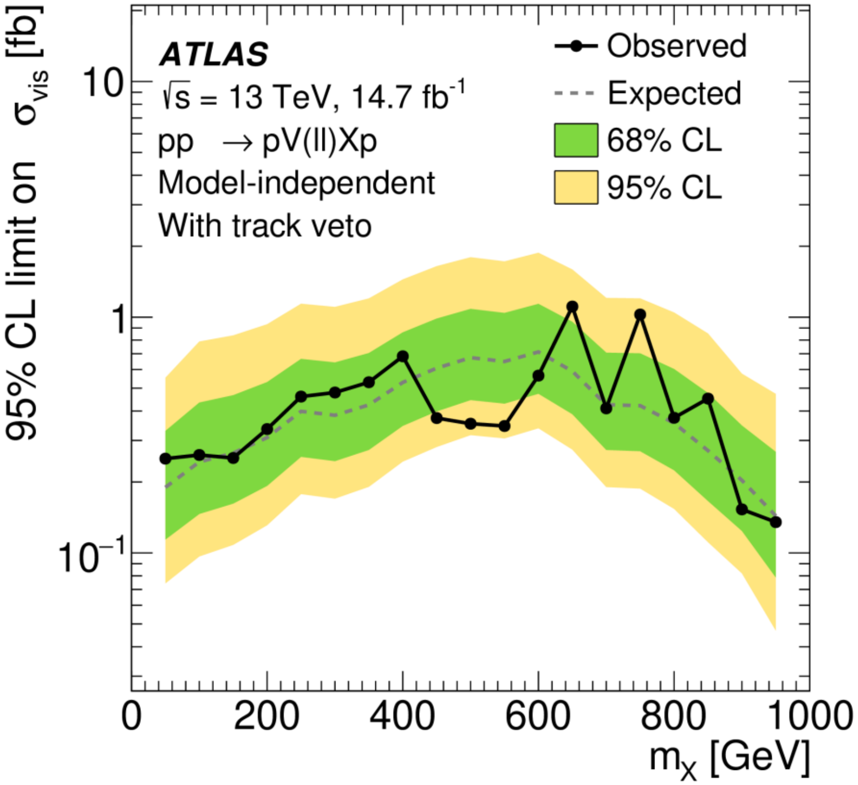

Exclusive limits obtained down to below 1 fb!
High level of sensitivity to a wide range of potential BSM physics

Paper in JHEP Coming Soon!

Paper now publicly available in arXiv! [2603.20837]
Accepted by JHEP in June and awaiting publication!

- Full analysis team:

Adrien Auriol[a], Maura Barros[b], Peter Bussey[c], Nuno Castro[b], Dave Charlton[d], Aleksandra Dimitrievska[d], Andrew Kirk[d], Josh Lomas[d], Viktoriia Lysenko[e], Paul Newman[d], Ferhat Ozturk[f], Andre Sopczak[e], Rafal Staszewski[f], Marek Tasevsky[g]

[a]*Laboratoire de Physique de Clermont-Ferrand (LPC),* [b]*Laboratório de Instrumentação e Física Experimental de Partículas (LIP),* [c]*University of Glasgow,* [d]*University of Birmingham,* [e]*IEAP CTU in Prague,* [f]*Institute of Nuclear Physics Polish Academy of Sciences,* [g]*Institute of Physics of the Czech Academy of Sciences*

EUROPEAN ORGANISATION FOR NUCLEAR RESEARCH (CERN)

Submitted to: JHEP

CERN-EP-2025-284
24th March 2026

Missing-mass search in forward-proton-tagged dilepton events with the ATLAS detector

The ATLAS Collaboration

A search is conducted in proton–proton collisions at the Large Hadron Collider for photon-induced production $pp \to pp + \gamma\gamma$, $(\gamma\gamma \to VX)$ of a visible particle V decaying into a pair of same-flavour charged leptons (e^+e^- or $\mu^+\mu^-$) and an undetected invisible component X. Measurements of the outgoing proton energies by the ATLAS forward proton spectrometer allow the full photon–photon four-momentum to be reconstructed. By subtracting the visible four-momentum of the central system measured with the ATLAS detector, the 'missing mass' of any event components not detected in the central region can be reconstructed, enabling the reconstruction of X without knowing its properties, thus allowing the search to be model-independent. A search for a narrow resonance is performed in the missing-mass spectrum between 100 GeV and 900 GeV. The analysis uses data collected in 2017 from proton–proton collisions at a centre-of-mass energy of $\sqrt{s} = 13$ TeV, corresponding to an integrated luminosity of 14.7 fb^{-1}. No significant excess over the Standard Model expectation is observed and upper limits at 95% confidence level are set on the fiducial cross sections for three different signal models in the range between 128 and 2.5 fb. Additionally, model-independent limits are set on the visible cross section of BSM processes, for two sets of selection criteria. Both individual lepton flavour decay channels of the visible boson and a combination of the two channels are considered.

Summary

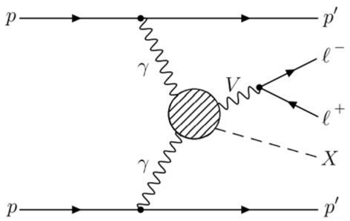

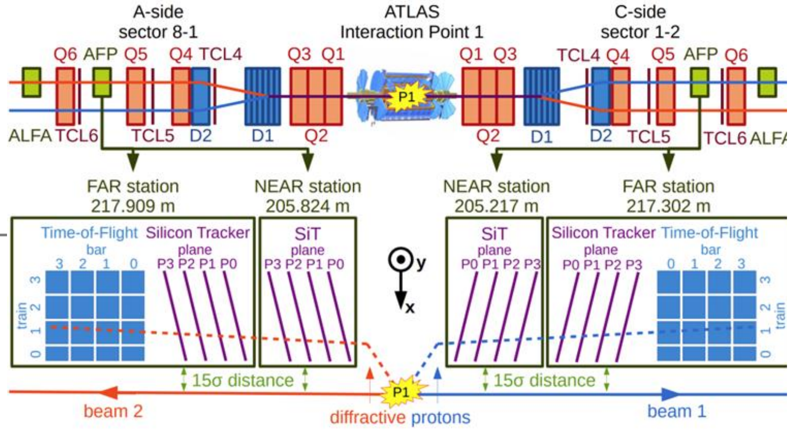

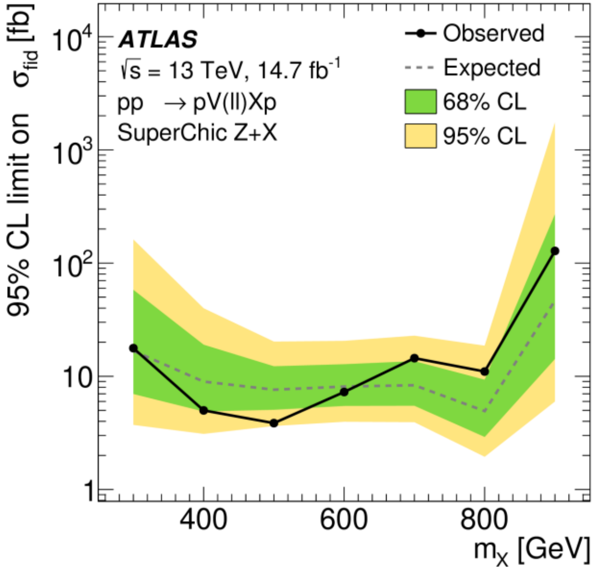

The first ATLAS analysis to **search for BSM physics** by reconstructing the **missing mass spectrum** using **AFP**

- **Three independent signal models** tested, with varying kinematics
- Very high background suppression achieved using **track veto selection** to significantly improve sensitivity
- **Data-driven background model** using event mixing of central (ATLAS) and proton (AFP) event components – validated using MC
- Dominant systematics from **AFP and background normalisation**
- Obtained O(10 fb) upper limits on **signal cross section** for all models
  - Additional **model-independent limits** on the visible cross section for BSM physics obtained down to ~1 fb

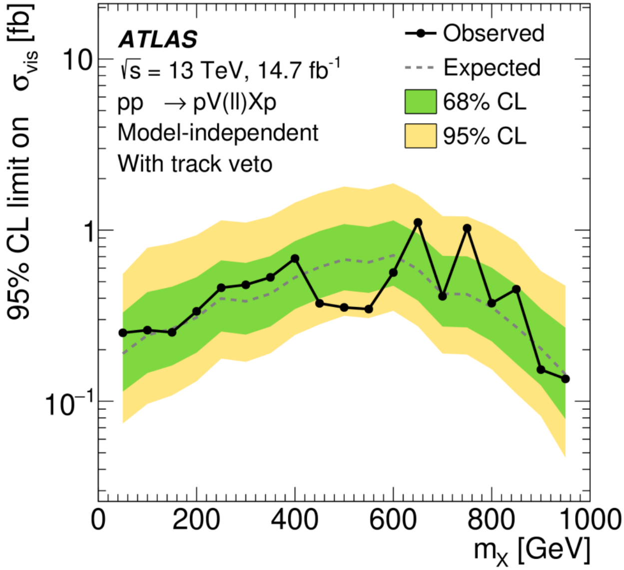

Paper now publicly available in arXiv! [2603.20837]
Accepted by JHEP in June and awaiting publication!

- Up to **280 fb^{-1}** of data recorded in **Run 3** for a future version of this analysis!

Back-up

AFP Simulation

- Dedicated **fast simulation** developed separated from central ATLAS simulation:
  - Simulates transport of truth-level protons through LHC beam optics to AFP
  - **Kinematic smearing** applied to simulate reconstruction resolution in AFP

  - Can be simulated down to silicon hit clusters or tracks

Signal Kinematic Comparison

- **Kinematic comparison** between signal models with m_X = 500 GeV at **reconstructed level:**

Dilepton p_T

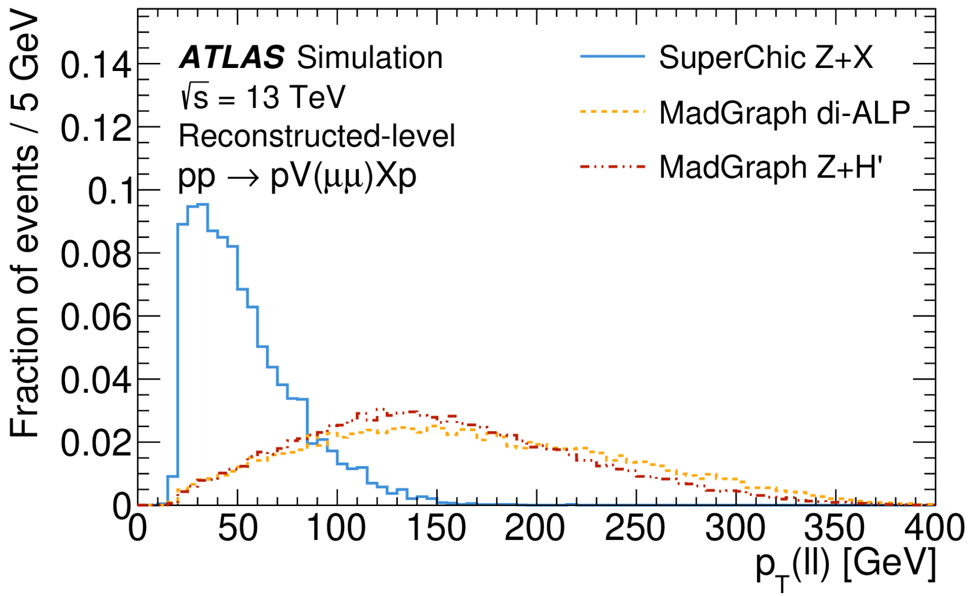

Proton ξ

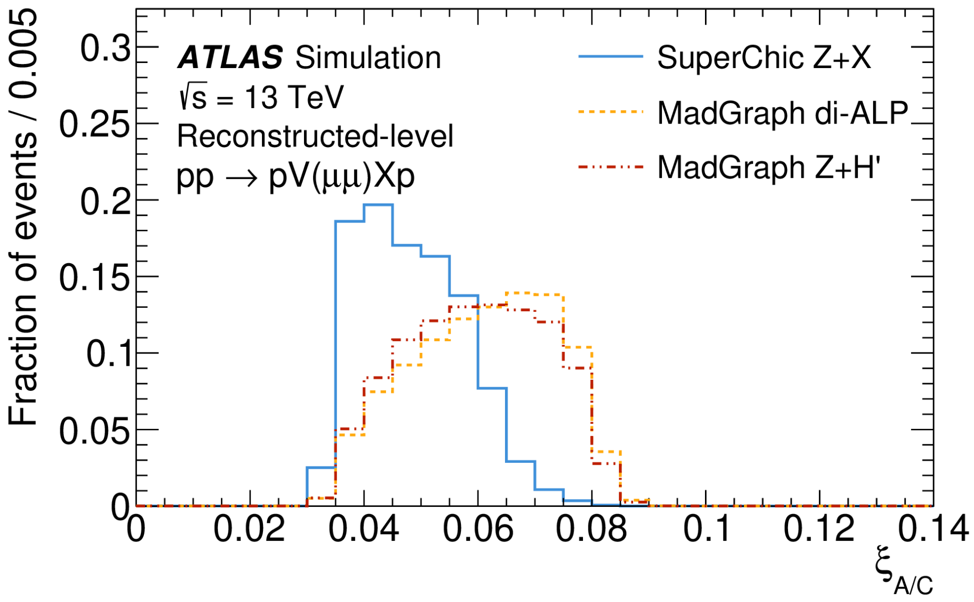

- Proton ξ range highly restricted by reconstructed-level selections

Wide range of phase space covered by the three models

Object Selection

Selections applied to **physics objects** used in analysis:

Feature	Electron/Muon Event Criterion
p_{T}	$> 18/15$ GeV
$\lvert\eta\rvert$	$< 2.47/2.4$
Identification	Loose
Isolation	Loose
$\left\lvert d_0^{\mathrm{BL}}\right\rvert / \sigma\left(d_0\right)$	$< 5/3$
$\left\lvert\Delta z_0^{\mathrm{BL}} \sin\theta\right\rvert$	< 0.5
Proton quality	Medium
Proton ξ	$0.02 < \xi < 0.12$
Proton reconstruction	Single or double-station

Track-to-vertex association cuts

Single-station reconstruction is less precise proton reconstruction used when there is only a single track in the FAR station

Background Validation with MC

Create secondary background model using MC simulation to validate data-driven model

- Simulate central SM processes
- Overlay database of randomly assigned pile-up protons taken from 2017 data
- Model fake lepton contribution using same-sign lepton selection on data

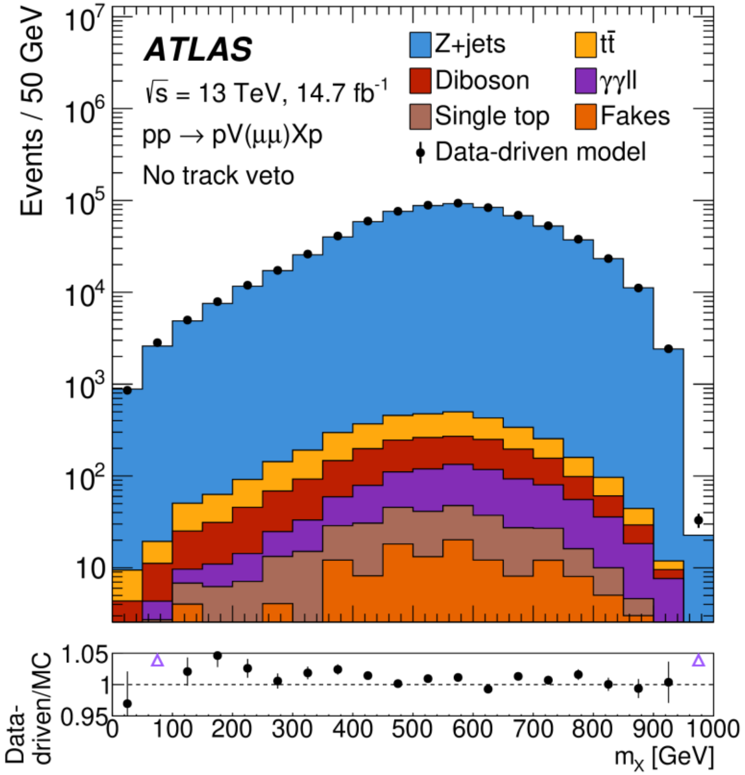

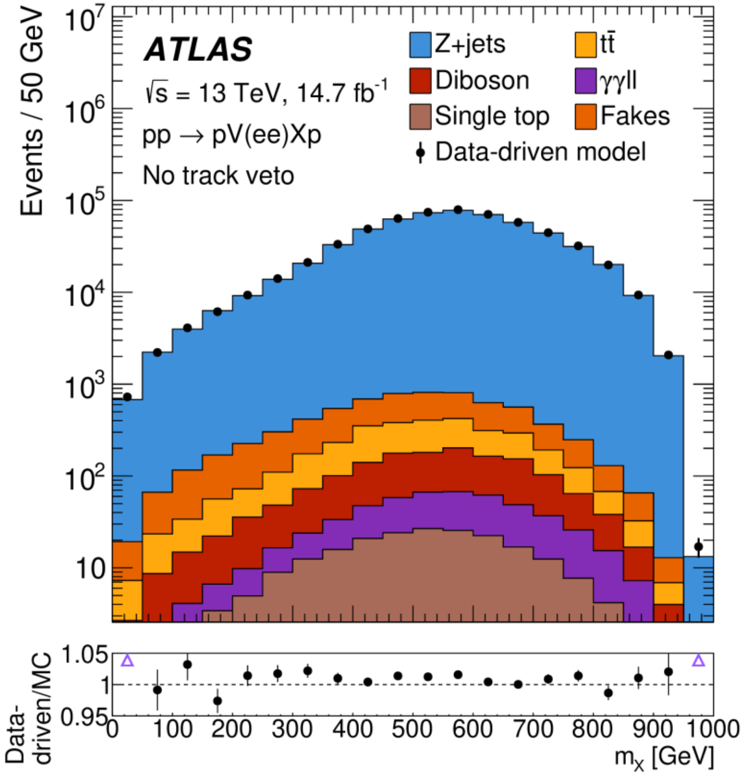

Excellent agreement observed
Data-driven model validated for use in final fits

Background Track Veto Effect

Estimated effect on the background composition after applying the track veto

- Quark-induced backgrounds with additional underlying event activity are heavily suppressed
- Exclusive photon-induced backgrounds become as large as Z+jets
- Distributions are normalised due to known mismodelling of underlying event

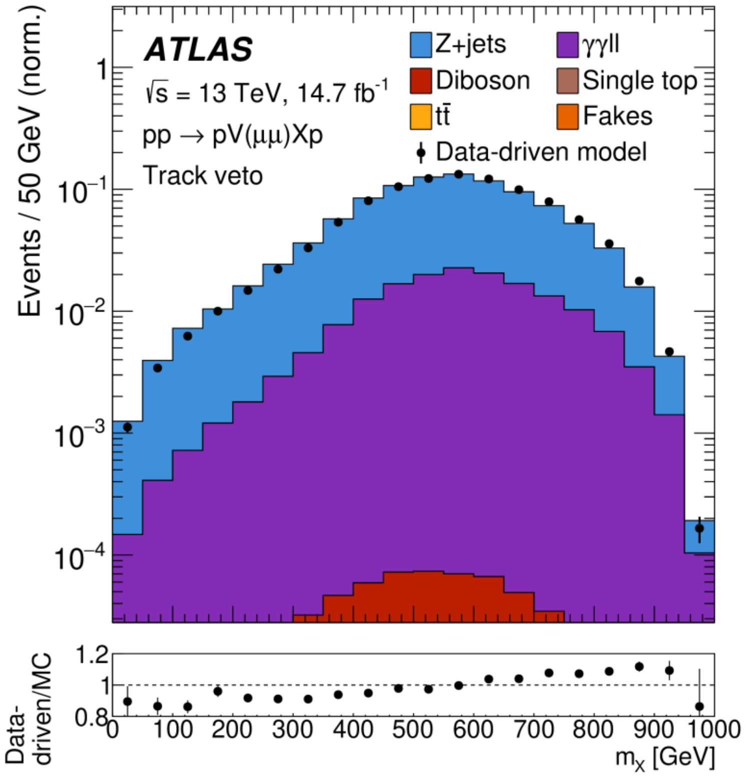

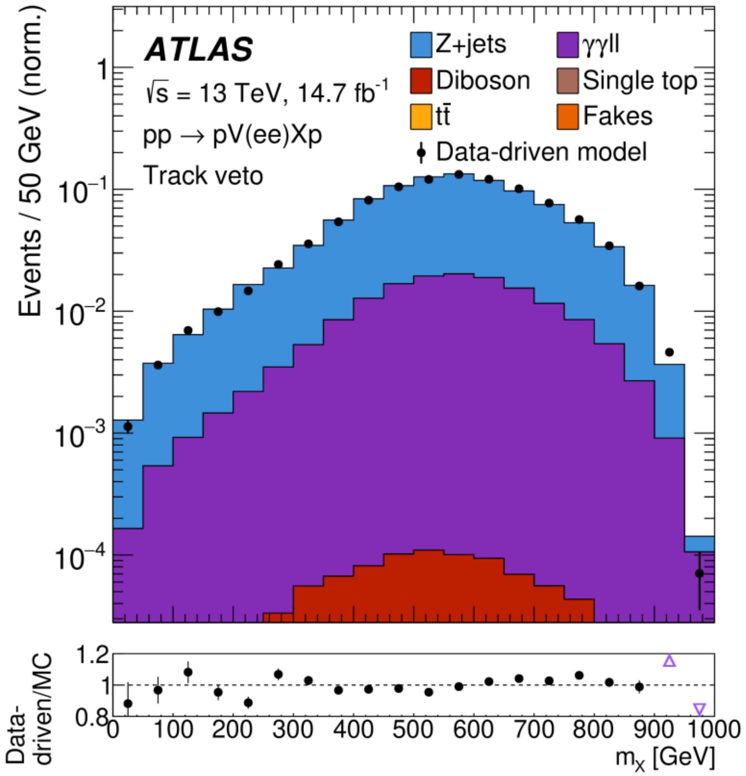

Good agreement still observed
Comparison is less direct due to modelling issue

Track Veto Signal Efficiency Closure

- Comparison between closure study in **muon** and **electron** channels

Muon Channel

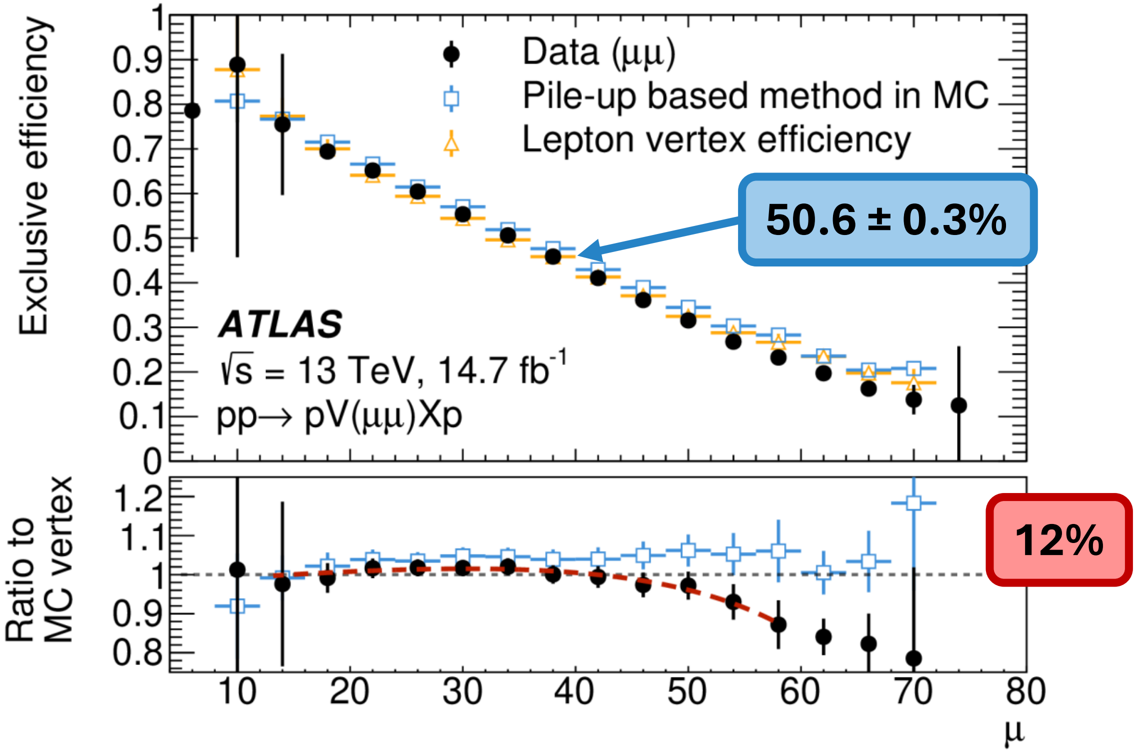

Electron Channel

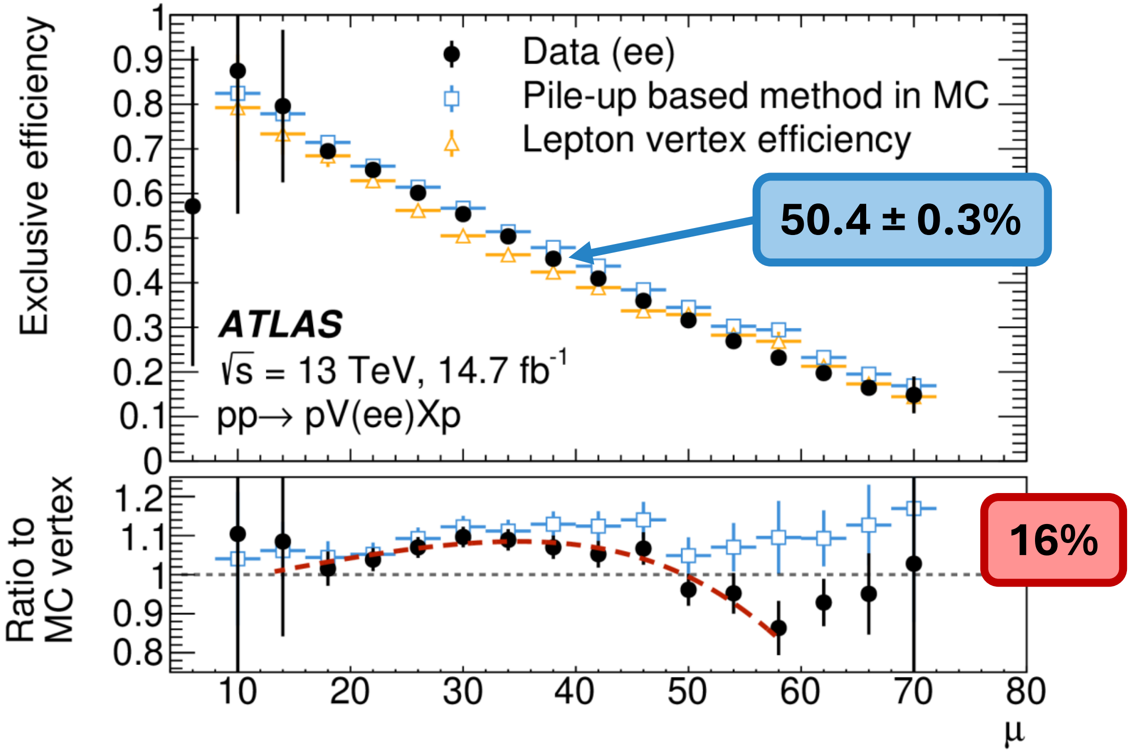

- Higher uncertainty observed in electron channel
  - Attributed to Bremsstrahlung emission from signal electrons and larger effects from track-to-vertex matching requirements, due to poorer *ee* vertex resolution

Systematics – Central

Several systematic uncertainties relating to the central event are considered

Uncertainty	Effect on event yield		
	Signal		
Signal model	SuperChic	MadGraph di-ALP	MadGraph $Z + H'$
Track veto signal efficiency	16.1%	16.1%	16.1%
Pile-up reweighting	3.1%–4.6%	3.6%–4.4%	3.7%–4.4%
Luminosity	1.2%	1.2%	1.2%
Electron energy scale	4.0%–5.3%	3.9%–5.8%	3.6%–4.5%
Electron resolution	3.9%–5.3%	3.9%–5.8%	3.6%–4.5%
Electron trigger efficiency	0.6%–0.7%	0.6%–0.7%	0.6%
Electron isolation efficiency	0.6%–0.7%	0.5%–0.7%	0.5%–0.6%
Electron trigger scale factor	0.6%–0.7%	0.5%–0.7%	0.5%–0.6%
Electron reconstruction efficiency	0.0%–0.7%	0.1%–0.7%	0.1%–0.6%
Electron ID efficiency	0.0%–0.7%	0.0%–0.7%	0.0%–0.6%
Muon energy scale	3.9%–5.2%	3.8%–5.7%	3.6%–5.5%
Muon resolution	3.8%–5.2%	3.8%–5.7%	3.6%–5.7%
Muon momentum scale	3.8%–5.2%	3.8%–5.7%	3.5%–5.5%
Muon trigger efficiency	0.2%–0.7%	0.0%–0.7%	0.0%–0.7%
Muon isolation efficiency	0.3%–0.6%	0.0%–0.6%	0.0%–0.5%
Muon reconstruction efficiency	0.1%–0.5%	$< 0.5\%$	$< 0.5\%$

All standard electron/muon uncertainties relating to MC considered for signal samples

Uncertainty on signal efficiency of track veto

Taken from difference between estimates obtained using two different methods

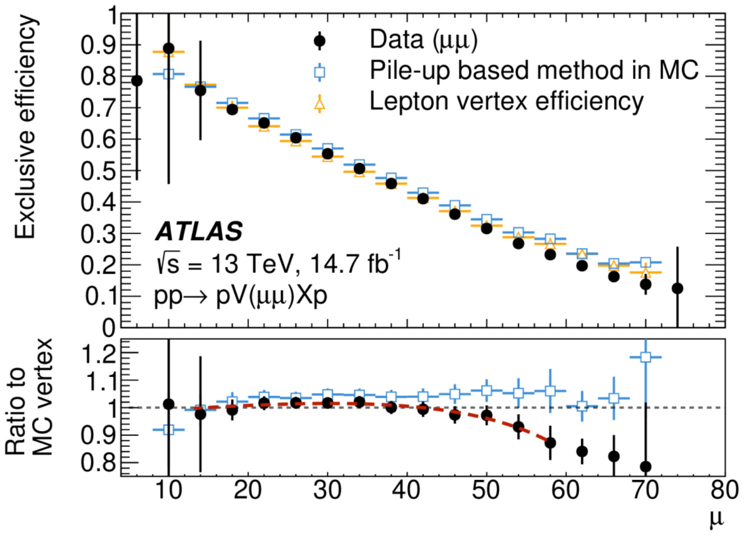

Systematics – Forward

Several systematic uncertainties relating to AFP and forward proton reconstruction are considered

Changes to proton reconstruction methodology

Track matching: decrease maximum transverse distance between proton tracks to 1 mm.
Track finding (distance): decrease maximum cluster separation in track to 0.4 mm
Track finding (clusters): increase minimum clusters in track to 3
Cluster neighbouring: expand search for neighbouring hits to include y direction

Uncertainty	Effect on event yield		
	Signal		
Signal model	SuperChic	MadGraph di-ALP	MadGraph $Z + H'$
AFP proton transport	8.8%–70.3%	15.7%–43.1%	13.3%–49.8%
AFP global alignment	5.7%–63.5%	12.2%–43.3%	11.2%–53.9%
AFP smearing	4.8%–37.7%	8.7%–22.0%	7.6%–24.8%
AFP reconstruction efficiency	3.2%–3.7%	2.7%–3.7%	3.4%–3.7%
AFP track matching	1.2%–2.5%	1.3%–1.8%	1.3%–1.6%
AFP track finding	0.6%–1.2%	< 0.5%	0.5%

Large variation in dominant proton systematics across signal mass range
e.g. proton transport:

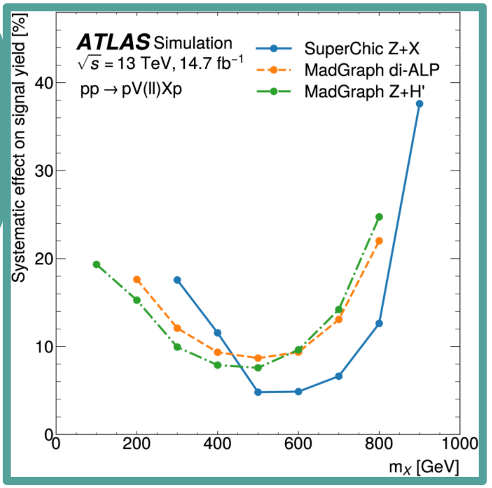

Verified expected effects on data

Uncertainties in simulation

Proton transport: Modifies beam slope by ±50 μrad
Global alignment: Modifies global alignment of AFP stations by ±300 μm in x
Smearing: Modifies width of distribution used to smear truth-level proton data by ±0.05 mm
Reconstruction efficiency: measured at 92 ± 2%

Systematics – Modelling

- Several sources of background modelling uncertainty considered:
  - Statistical uncertainty estimated with bootstrapping = **1%**
  - Pile-up distribution - **negligible**
    - Variation in interactions per bunch crossing across the dataset
  - Single-diffractive backgrounds - **negligible**
    - Effect on mixing strategy (single vs double-sided) on background shape
  - Pile-up variation in event-mixing - **negligible**
    - Difference in pile-up between each component of mixed background

- Signal modelling uncertainties
  - FSR, parton showering – **negligible**
  - Soft-survival probability (next slide)

Data and Background Model Comparison

- Comparison between **data** and **background model**
  - Only **preselection requirements** applied
  - Dilepton pair p_T, dilepton mass m_{ll}, proton ξ and missing mass m_X
  - Compared to expectations for a **500 GeV SuperChic Z+X signal** with a cross section of 50 fb (+**additional overlay** with signal scaled up by a factor of 10,000)

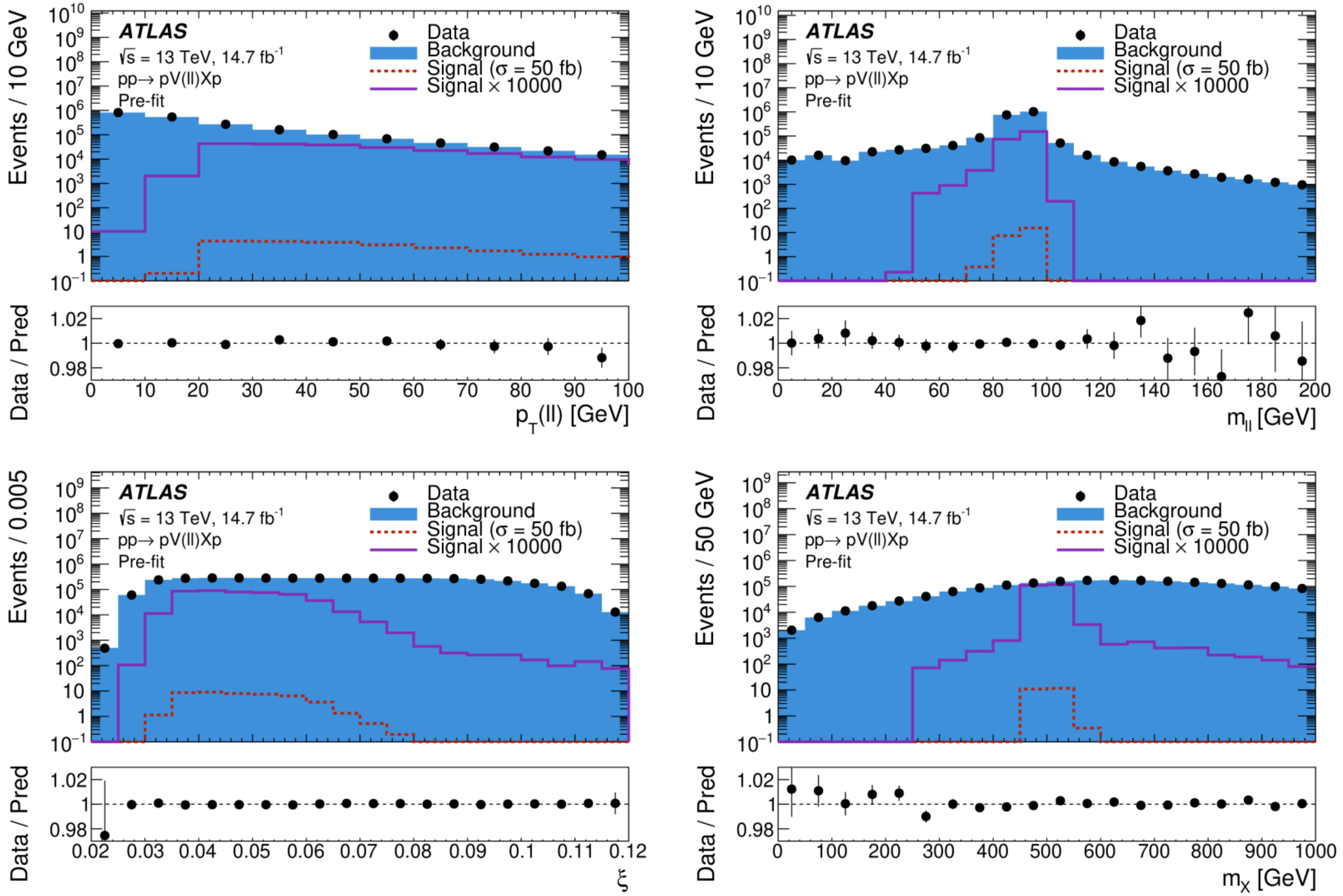

Data and Background Model Comparison

- Comparison between **data** and **background model**
  - **All signal region requirements** applied
  - Dilepton pair p_T, dilepton mass m_{ll}, proton ξ and missing mass m_X
  - Compared to expectations for a **500 GeV SuperChic Z+X signal** with a cross section of 50 fb (+**additional overlay** with signal scaled up by a factor of 100)

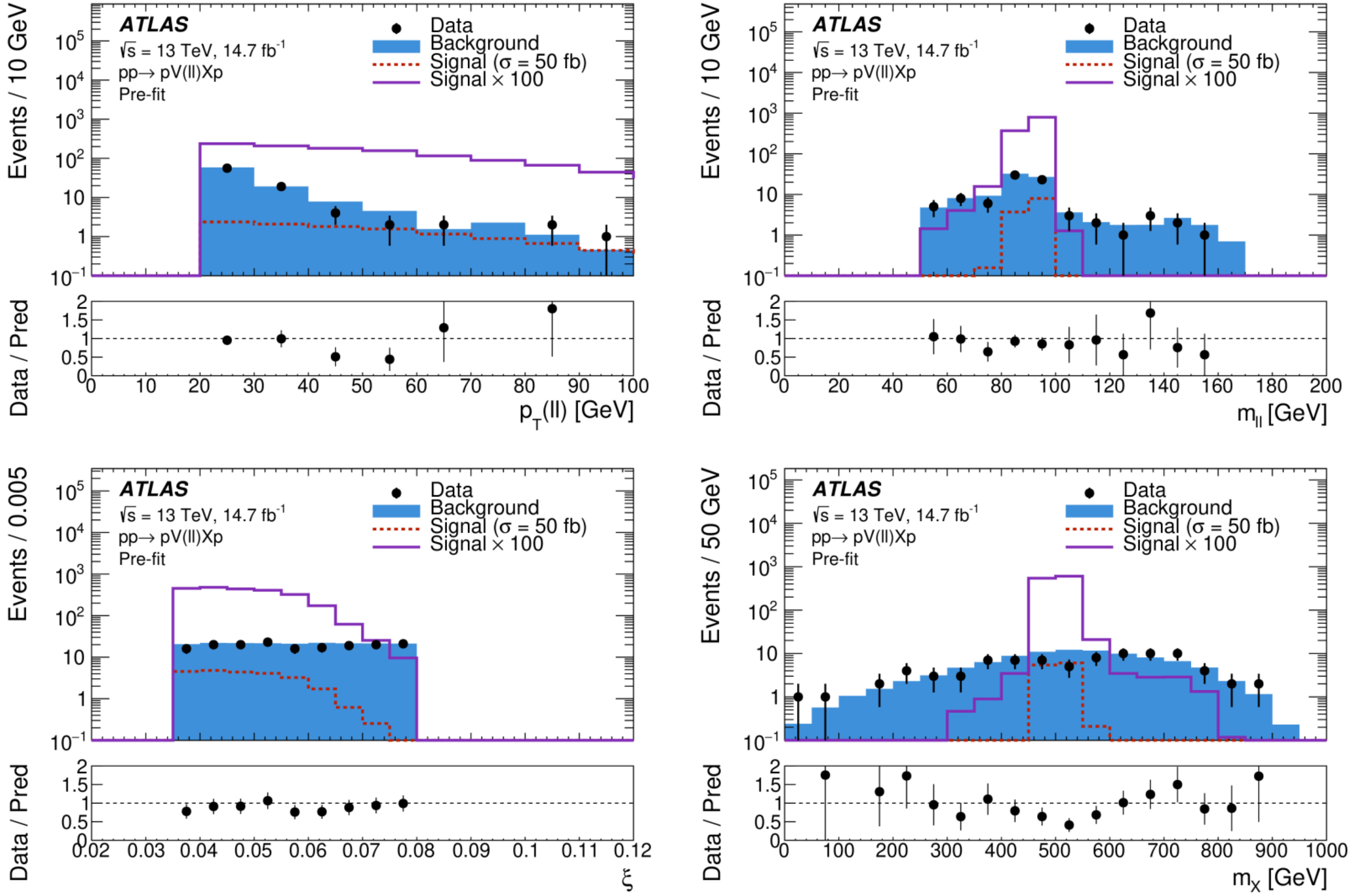

Acceptance × Efficiency

- Acceptance times efficiency for each signal model with respect to the full signal selection, including the track veto and mass window, relative to events passing the fiducial selection:

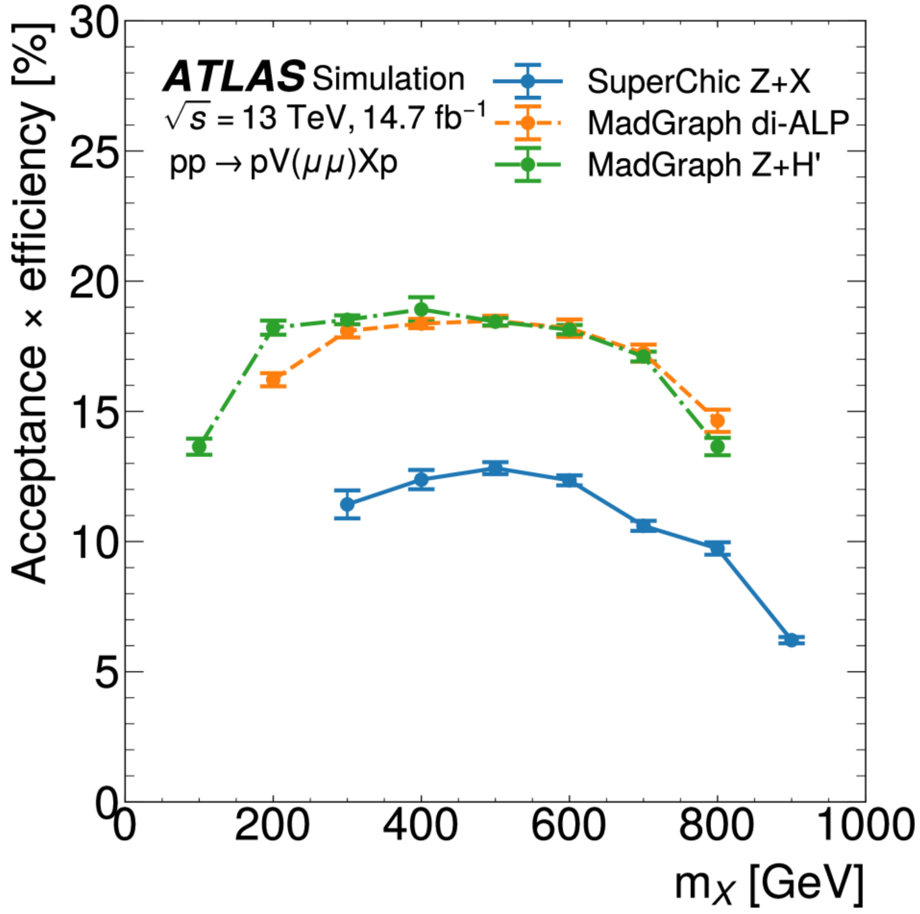

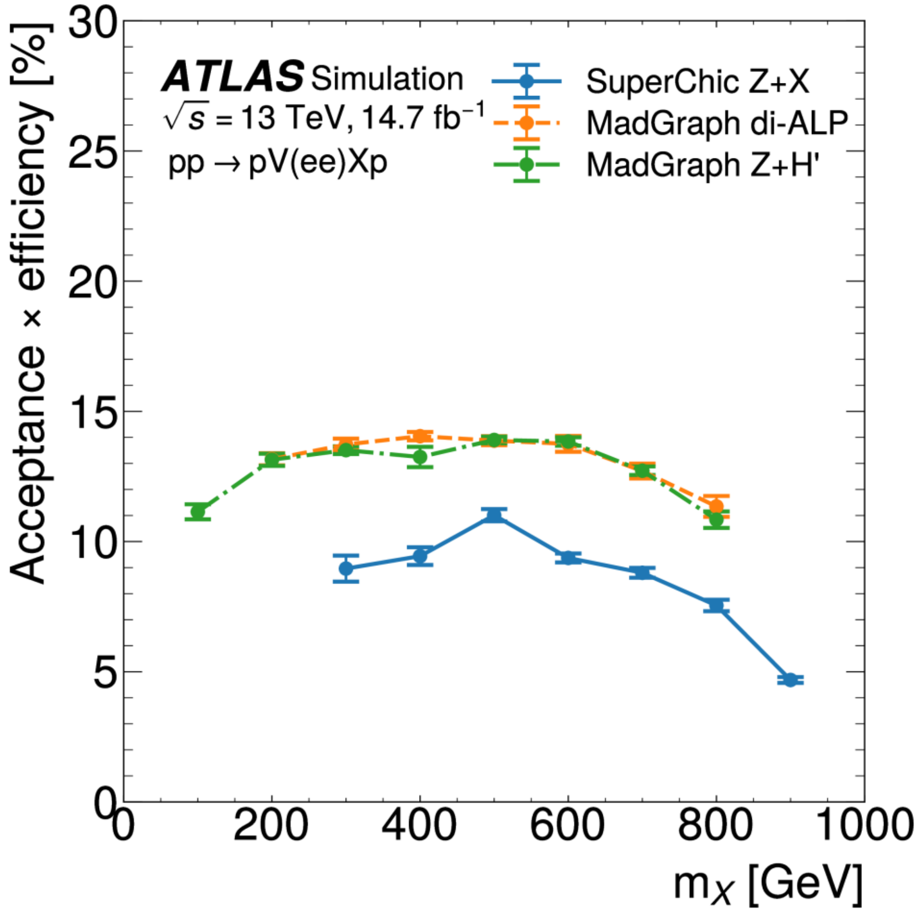

Mismatched Signal Proportions

- Proportion of simulated signal events within the mass window applied at each hypothesised signal mass, which fall outside the fiducial selection:

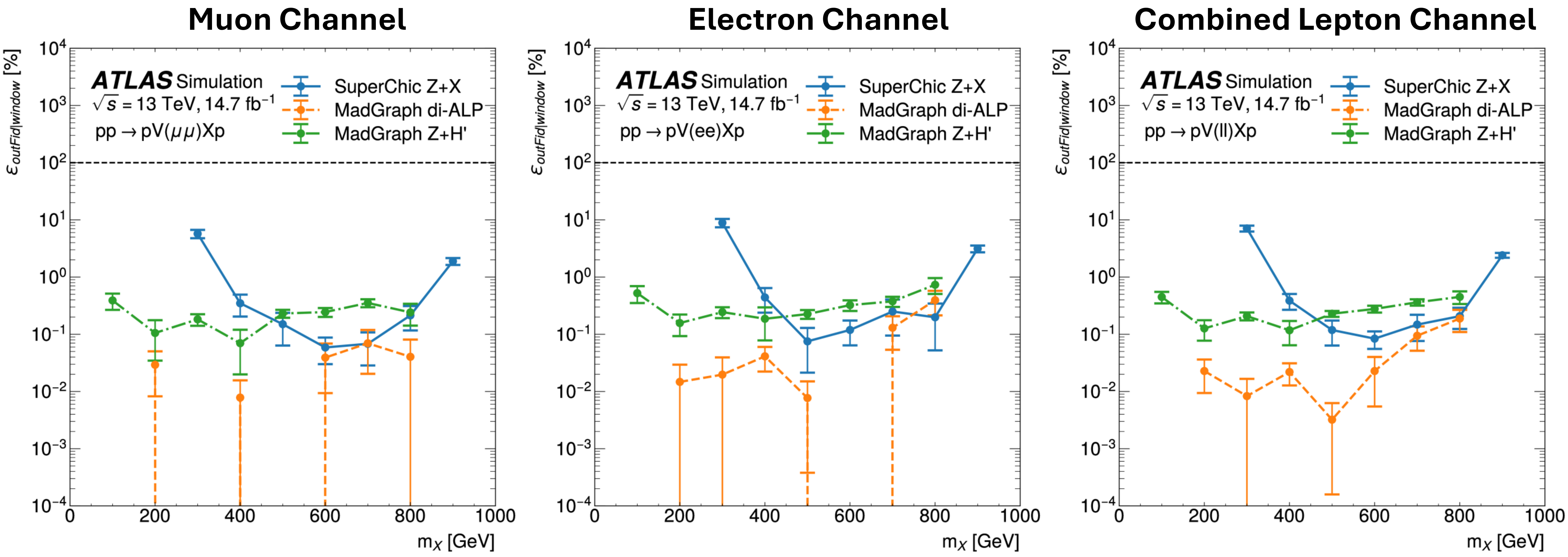

Mismatched Signal Proportions

- Systematic ranking plots for each signal model with m_X = 500 GeV, in the combined lepton channel

SuperChic Z+X

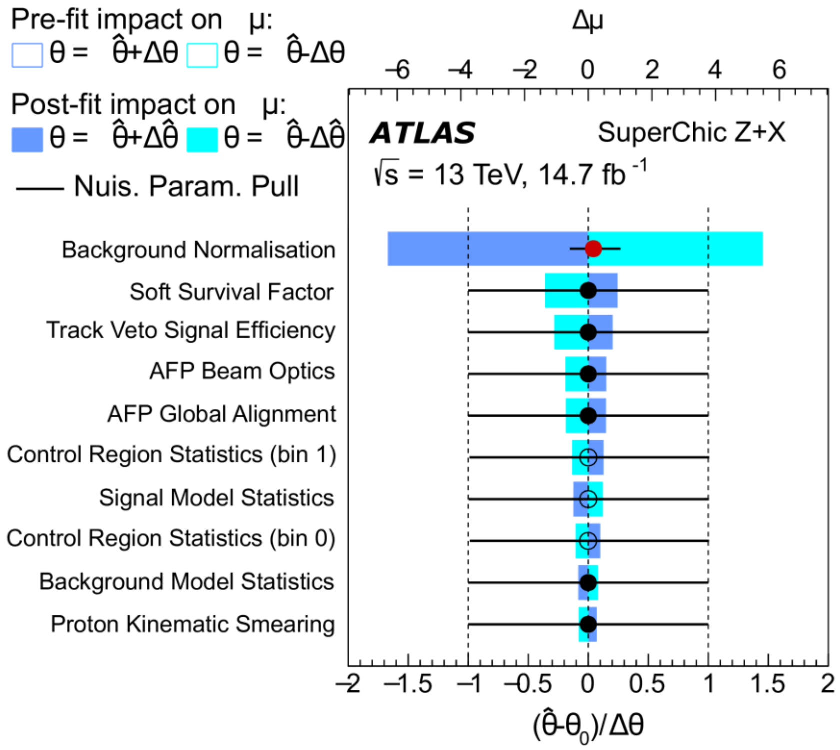

MadGraph di-ALP

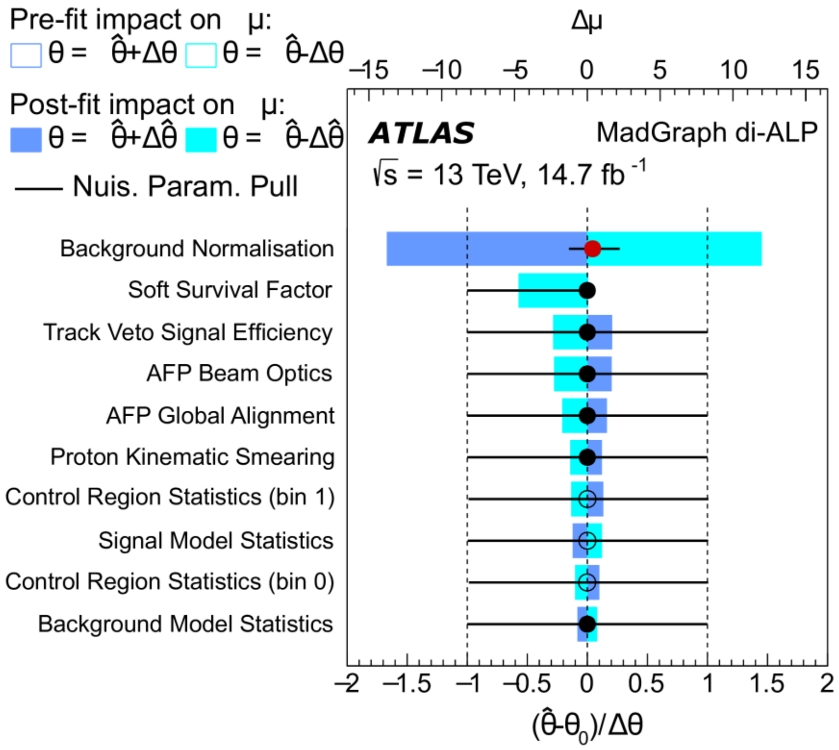

MadGraph Z+H'

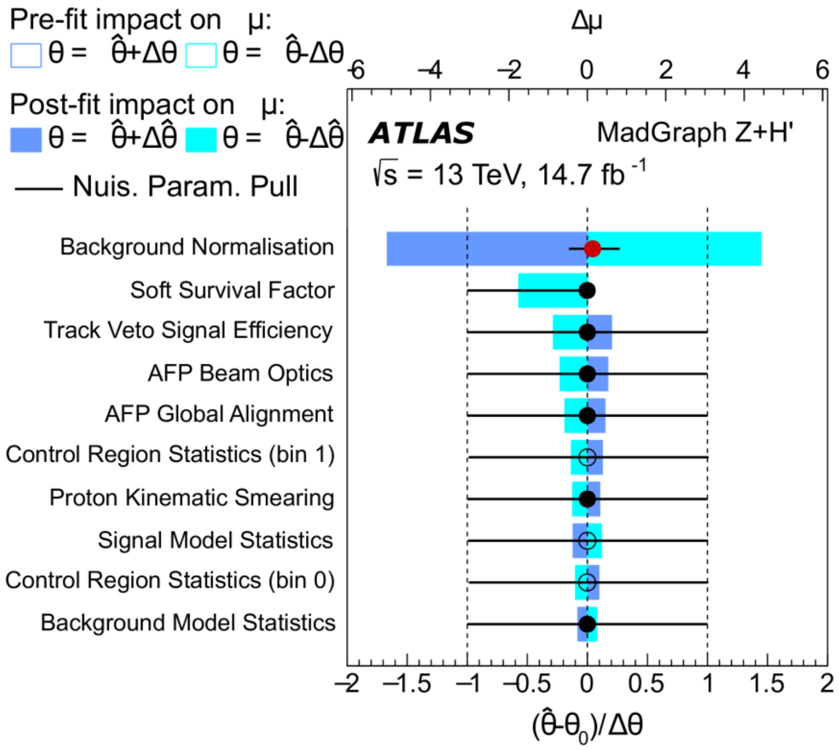

➤ Soft-survival, track veto efficiency and AFP optics and alignment consistently highest ranked

Soft-Survival - Uncertainty

arXiv:1708.04053

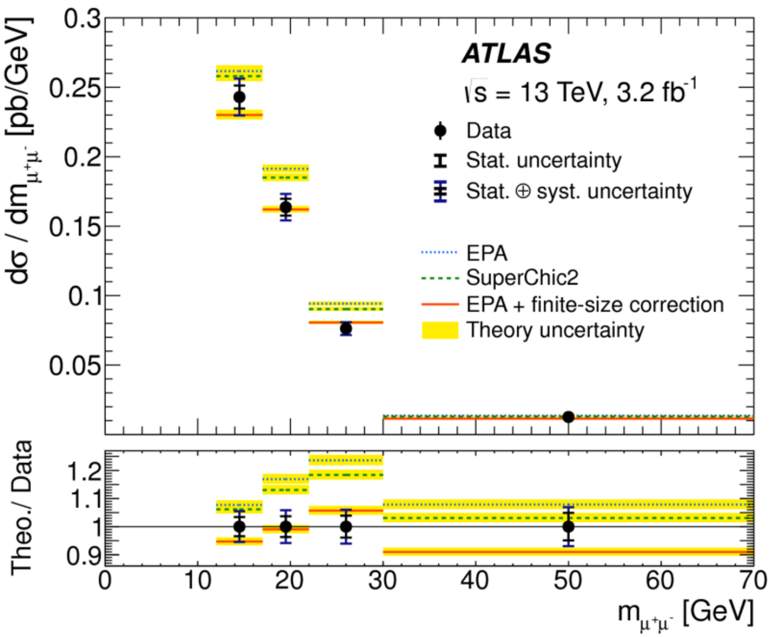

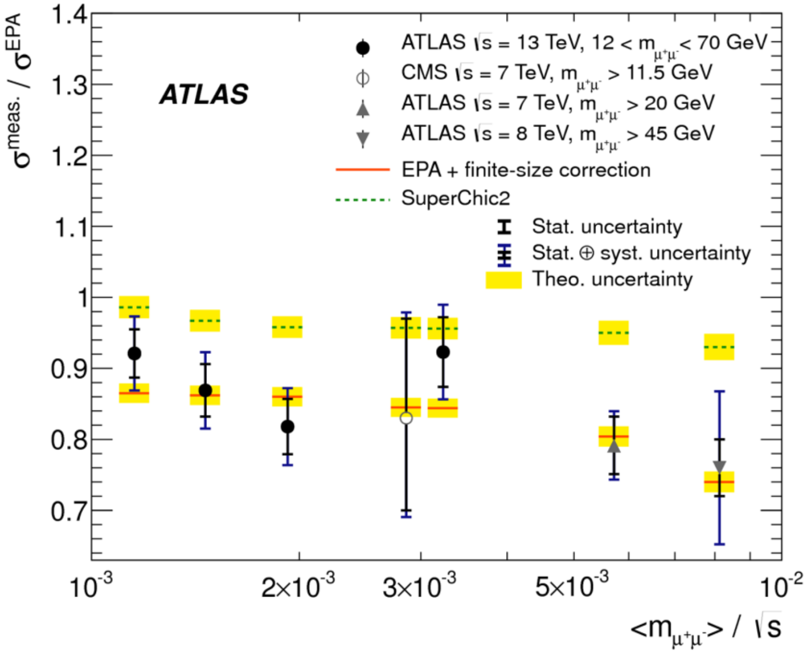

- Di-muon exclusive production differential cross-section measurements
  - Maximum deviation of around 20%

arXiv:2009.14537

Di-lepton + AFP paper

TABLE I. Fiducial cross sections from the combined HERWIG and LPAIR predictions with $S_{\rm surv} = 1$ and $S_{\rm surv}$ estimated using Refs. [33,34] as described in the main text. SUPERCHIC 4 [97] predictions include fully kinematically dependent $S_{\rm surv}$. Uncertainties of 7% (17%) are assigned for predictions of the exclusive (single-dissociative) processes [98]. The bottom row displays the measured cross sections with statistical and systematic uncertainties combined.

$\sigma_{\rm HERWIG+LPAIR} \times S_{\rm surv}$	$\sigma^{\rm fid.}_{ee+p}$ (fb)	$\sigma^{\rm fid.}_{\mu\mu+p}$ (fb)
$S_{\rm surv} = 1$	15.5 ± 1.2	13.5 ± 1.1
$S_{\rm surv}$ using Refs. [33,34]	10.9 ± 0.8	9.4 ± 0.7
SUPERCHIC 4 [97]	12.2 ± 0.9	10.4 ± 0.7
Measurement	11.0 ± 2.9	7.2 ± 1.8

- Average deviation also around 20% across the two channels

CMS Fiducial Selection

- CMS also set their limits relative to a fiducial volume defined by the following selection:

Table 1: Combined CMS+CT-PPS fiducial volume selection criteria in the Z and γ analyses. The leading- and subleading-p_{T} leptons, where p_{T} is transverse momentum, are labelled as ℓ_1 and ℓ_2, respectively. The Z boson mass is noted as m_{Z}.

Selection/analysis	$\mathrm{Z} \to \mathrm{e}^+\mathrm{e}^-/\mathrm{Z} \to \mu^+\mu^-$	γ
	$\geq$2 same-flavour leptons (e or μ)	
	opposite electric charge	
Leptons/photons	$p_{\mathrm{T}}(\ell_1) > 30\,\mathrm{GeV}$, $\lvert\eta(\ell_1)\rvert < 2.4$	1γ within $\lvert\eta(\gamma)\rvert < 1.44$
	$p_{\mathrm{T}}(\ell_2) > 20\,\mathrm{GeV}$, $\lvert\eta(\ell_2)\rvert < 2.4$	
	$\lvert m(\ell_1, \ell_2) - m_{\mathrm{Z}}\rvert < 10\,\mathrm{GeV}$	
Boson p_{T}	$p_{\mathrm{T}}(\mathrm{Z}) > 40\,\mathrm{GeV}$	$p_{\mathrm{T}}(\gamma) > 95\,\mathrm{GeV}$
Protons	$0.02 < \xi_+^{\mathrm{gen}} < 0.16$ and $0.03 < \xi_-^{\mathrm{gen}} < 0.18$	

- In our original comparison we were using a much wider fiducial volume (no cuts except $\xi < 0.15$) so our results look worse by comparison – we can calculate the conversion

CMS Model Comparison

- The models are based on equivalent parameterisations:

SuperChic

The signal is generated using a simplified model in which a system ZX is produced in an elastic photon-induced process, where X is an invisible particle with mass m_X. This process is implemented in SuperChic version 5.1 and it was hadronised using Pythia8 version 8.310. The mass of the VX system is generated proportional to $e^{-\tau . m_{VX}}$. The model takes as input m_X and τ. m_X is varied between 300 GeV and 1000 GeV and τ is defined as 0.04 GeV^{-1}. This value of τ follows what was done in the CMS published analysis CMS-PAS-EXO-19-009 [3]. However, it was verified that the exact value of τ does not significantly influence the process's kinematics. Z decays into electrons and muons are considered. The tauonic decay is

CMS Model

The signal is simulated using a simplified MC model that uses as main inputs the mass of the X particle, m_X, and the p_z spectrum of the VX system, where $V = Z, \gamma$. It is assumed that the vector boson V is produced isotropically in the VX frame, and that the leptons from the Z decay are also produced isotropically in the Z reference frame. Samples are produced for a range of m_X values, with the requirement that the corresponding mass of the VX system (m_{VX}) falls within the acceptance of CT-PPS. For each event, the m_{VX} is generated assuming an exponential spectrum, $m_{VX} = m_X + \varepsilon + 100\,\text{GeV}$, where ε is a randomly distributed variable following an exponential probability distribution function with decay constant $\tau = -0.04\,\text{GeV}^{-1}$. The

- CMS generator-level distribution (applied corrections to account for detector inefficiency):

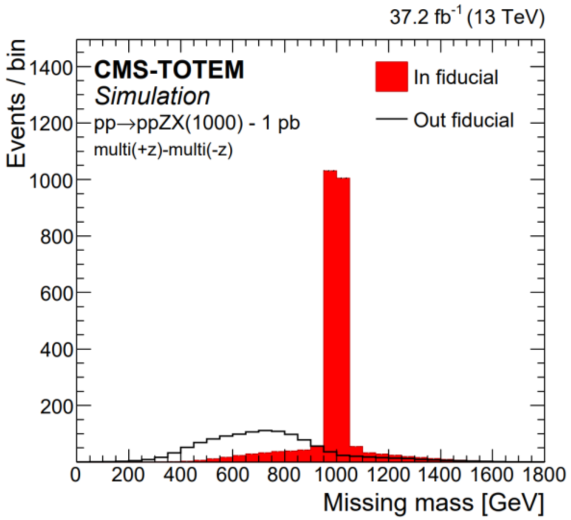

- CMS signal in/outside of fiducial volume
- Smeared tail due to insertion of pile-up protons (similar to our simulation)

Model Independent Limit Tables

Model-independent limits for a range of generic signals, both with and without the track veto selection applied:

Without track veto

Signal region [GeV]	Data	Expected	σ_{vis} [fb]	$S^{0.95}_{obs}$	$S^{0.95}_{exp}$	p_0 (Z)
$m_X \in [25, 75)$	1349	1437 ± 16	2.8	42	81^{+114}_{-58}	0.50 (0.0)
$m_X \in [75, 125)$	2994	3014 ± 33	7.7	114	126^{+177}_{-91}	0.50 (0.0)
$m_X \in [125, 175)$	4982	4925 ± 54	14.8	217	175^{+244}_{-126}	0.26 (0.6)
$m_X \in [175, 225)$	7410	7311 ± 82	21.0	309	234^{+327}_{-168}	0.20 (0.8)
$m_X \in [225, 275)$	10499	10660 ± 120	15.1	222	308^{+429}_{-222}	0.50 (0.0)
$m_X \in [275, 325)$	15746	15360 ± 170	49.6	730	411^{+571}_{-296}	0.03 (1.8)
$m_X \in [325, 375)$	23142	23260 ± 250	33.7	496	569^{+790}_{-410}	0.50 (0.0)
$m_X \in [375, 425)$	34478	34410 ± 360	57.5	845	799^{+1109}_{-576}	0.50 (0.0)
$m_X \in [425, 475)$	44813	45390 ± 470	46.9	689	991^{+1376}_{-715}	0.50 (0.0)
$m_X \in [475, 525)$	53807	53870 ± 560	77.4	1138	1180^{+1637}_{-851}	0.50 (0.0)
$m_X \in [525, 575)$	58189	58380 ± 610	79.5	1169	1287^{+1785}_{-929}	0.50 (0.0)
$m_X \in [575, 625)$	55107	55010 ± 580	88.2	1296	1229^{+1706}_{-887}	0.44 (0.2)
$m_X \in [625, 675)$	45876	45720 ± 500	76.8	1129	1025^{+1423}_{-739}	0.39 (0.3)
$m_X \in [675, 725)$	35959	35850 ± 370	60.3	887	815^{+1130}_{-587}	0.40 (0.3)
$m_X \in [725, 775)$	26635	26300 ± 270	59.5	875	618^{+860}_{-445}	0.15 (1.1)
$m_X \in [775, 825)$	17448	17300 ± 180	36.7	539	433^{+601}_{-312}	0.25 (0.7)
$m_X \in [825, 875)$	9066	9200 ± 94	12.9	189	263^{+366}_{-189}	0.50 (0.0)
$m_X \in [875, 925)$	2901	3006 ± 31	5.0	73	124^{+173}_{-89}	0.50 (0.0)
$m_X \in [925, 975)$	178	165 ± 2	2.6	38	27^{+38}_{-19}	0.16 (1.0)

With track veto

Signal region [GeV]	Data	Expected	σ_{vis} [fb]	$S^{0.95}_{obs}$	$S^{0.95}_{exp}$	p_0 (Z)
$m_X \in [25, 75)$	1	0.39 ± 0.11	0.25	3.7	$3.0^{+4.8}_{-0.0}$	0.21 (0.8)
$m_X \in [75, 125)$	1	0.83 ± 0.23	0.26	3.8	$3.6^{+6.4}_{-0.6}$	0.43 (0.2)
$m_X \in [125, 175)$	1	1.14 ± 0.35	0.25	3.7	$3.9^{+6.9}_{-0.9}$	0.50 (0.0)
$m_X \in [175, 225)$	2	1.68 ± 0.61	0.34	4.9	$4.5^{+7.8}_{-1.5}$	0.42 (0.2)
$m_X \in [225, 275)$	4	3.19 ± 1.03	0.46	6.8	$5.9^{+9.8}_{-2.9}$	0.35 (0.4)
$m_X \in [275, 325)$	4	2.78 ± 0.94	0.48	7.0	$5.6^{+9.5}_{-2.6}$	0.28 (0.6)
$m_X \in [325, 375)$	5	3.62 ± 1.11	0.53	7.8	$6.2^{+10.4}_{-3.2}$	0.28 (0.6)
$m_X \in [375, 425)$	8	5.89 ± 1.59	0.68	10.0	$7.8^{+12.7}_{-4.8}$	0.25 (0.7)
$m_X \in [425, 475)$	6	10.82 ± 1.70	0.37	5.5	$8.9^{+14.5}_{-5.9}$	0.50 (0.0)
$m_X \in [475, 525)$	6	13.74 ± 2.44	0.35	5.2	$9.9^{+15.9}_{-6.5}$	0.50 (0.0)
$m_X \in [525, 575)$	5	12.52 ± 2.84	0.35	5.1	$9.5^{+15.3}_{-6.3}$	0.50 (0.0)
$m_X \in [575, 625)$	10	12.80 ± 2.91	0.57	8.3	$10.5^{+16.8}_{-7.0}$	0.50 (0.0)
$m_X \in [625, 675)$	13	6.53 ± 1.65	1.11	16.3	$8.7^{+14.1}_{-5.7}$	0.04 (1.8)
$m_X \in [675, 725)$	4	4.21 ± 1.01	0.41	6.0	$6.3^{+10.4}_{-3.3}$	0.50 (0.0)
$m_X \in [725, 775)$	10	3.42 ± 0.70	1.03	15.1	$6.2^{+10.3}_{-3.2}$	0.005 (2.6)
$m_X \in [775, 825)$	3	2.77 ± 0.47	0.37	5.5	$5.2^{+8.9}_{-2.2}$	0.45 (0.1)
$m_X \in [825, 875)$	3	1.19 ± 0.21	0.45	6.6	$4.0^{+7.0}_{-1.0}$	0.09 (1.4)
$m_X \in [875, 925)$	0	0.58 ± 0.01	0.20	3.0	$3.0^{+5.1}_{-0.0}$	0.50 (0.0)
$m_X \in [925, 975)$	0	0.05 ± 0.02	0.20	3.0	$3.0^{+4.0}_{-0.0}$	0.50 (0.0)